Soft Computing (2022) 26:13735–13764
https://doi.org/10.1007/s00500-022-07364-6

APPLICATION OF SOFT COMPUTING

Modeling the leader–follower supply chain network under uncertainty and solving by the HGALO algorithm

Javid Ghahremani Nahr[1] · **Anwar Mahmoodi**[1] · **Abdolsalam Ghaderi**[1]

Accepted: 6 July 2022 / Published online: 3 August 2022

Abstract

The purpose of this article is to develop a competitive supply chain network (SCN) in the face of uncertainty. The objective of the leader chain is to maximize total network profits by strategically locating suppliers, manufacturers, distribution centers, and retailers. Additionally, the follower chain seeks to maximize the network's profit. Both factors, optimal flow allocation to different echelons of the SCN and product pricing, are examined in the leader chain and follower chain. The KKT conditions are used in this article to convert a bi-level model to a one-level model. Additionally, a fuzzy programming technique is used to control the problem's uncertain parameters. According to the results obtained using the fuzzy programming technique, increasing the uncertainty rate increases demand while decreasing the OBFV and average selling price of products. Finally, the problem was untangled using a novel hybrid genetic and ant-lion optimization algorithm (HGALO). The results of problem solving in larger sizes demonstrate HGALO's superior efficiency in comparison with the other algorithm.

Keywords Leader–follower supply chain · KKT approach · HGALO algorithm · Stackelberg game

1 Introduction

A supply chain (SC) is a collection of independent companies that encompasses the entire process of acquiring and converting raw materials into finished goods, as well as maintaining, distributing, and transferring them to end customers. Nowadays, researchers emphasize competition both within and across chains (Zhang et al. 2017). Customer competition patterns have altered product and service supply chains, resulting in a shift in market competition between independent businesses and supply chains (Ghomi-Avili et al. 2018). There is a substantial body of literature on the SC design, the majority of which is devoted exclusively to the SC. Until now, the presence of competitors in SC, as well as their possible future emergence, has been inadequately considered. SC, on the other hand, competes for market share (Wang et al. 2016). As a result, even if there is no immediate competitor present, SC must be prepared for future competition (Saberi et al. 2018). Numerous studies have been conducted in the literature to evaluate games between different echelons of the SCN. A non-cooperative game is a type of game in which the buyer and seller compete for the highest possible profit margin (Li and Nagurney 2017). In a non-cooperative Stackelberg game, the strongest player assumes the role of leader and formulates his strategy first, followed by the follower (Yue and You 2017).

To address the aforementioned issue, a new model of the leader–follower network was developed with the goal of optimizing the profit of the leader and follower chains. As a result, this game can be classified as a distinct subgenre of Stackelberg. In the leader and follower SC, four echelons (suppliers, manufacturers, distribution centers, and retailers) are considered, and they compete for product pricing in the market (customers). Due to the uncertainty surrounding the amount of potential market demand, pricing in both leader and follower chains is extremely complicated. As a result,

✉ Abdolsalam Ghaderi
ab.ghaderi@uok.ac.ir

Javid Ghahremani Nahr
javidghahremani1369@gmail.com

Anwar Mahmoodi
anwar.mahmoodi@uok.ac.ir

[1] Department of Industrial Engineering, Faculty of Engineering, University of Kurdistan, Sanandaj, Iran

special tools such as fuzzy programming are used to control the potential demand parameters as well as the costs of product and raw material transportation between different echelons of the chain network (Szmelter-Jarosz et al. 2021; Nozari et al. 2022). The presence of strategic decisions in the leader chain is what distinguishes this paper's leader and follower chain networks. The location of facilities at all potential centers, such as suppliers, manufacturers, distribution centers, and retailers, should be made part of the leader chain's strategic planning. The optimal transport of products and raw materials between the two SCN echelons is a tactical decision in the leader and follower chains. Finally, operational decisions include pricing final products in the market (for customers) based on the leader and follower chains in order to make the most money in an uncertain environment.

The leader and follower members use the traditional (forward) SCN. As a result, a mathematical model of SC on two levels will be developed. In the paper presented here, we used the KKT technique to convert a bi-level mathematical model to a one-level mathematical model. Because location and SCN design problems are NP-Hard, this paper solves the problem using a novel combination of genetic algorithms (GA) and ant-lion optimization algorithms (ALO). The operators of the ant-lion optimization algorithm design the chromosome of the problem by locating potential facilities and allocating products optimally between different echelons of the leader and follower chains, whereas the genetic algorithm operators price the products in the market. Finally, statistical comparisons between the developed algorithm and other algorithms such as the genetic algorithm (GA), the ant-lion optimizer (ALO), the gray wolf optimizer (GWO), and the Harris-hawks optimizer (HHO) are made.

The article is structured as follows. The second section discusses the research background and the investigation of the research gap. The third section discusses the bi-level mathematical model of SCN. This section discusses a fuzzy programming technique for controlling uncertain parameters. The fourth section presents a novel combination of GA and ALO algorithms, as well as the initial chromosome design, for the problems of facility location, optimal product flow allocation, and market pricing of products. The fifth section investigates exact and meta-heuristic solution methods, as well as statistical comparisons, in small and large instances. The sixth section will examine the presentation of the research findings and recommendations for future research.

2 Literature review

Numerous studies have concentrated on the presentation of competitive single- and multi-product games between different SCN echelons as well as product pricing within each firm. Wu et al. (2012) examined five different power scenarios for a one-seller, two-buyer SC: (1) The seller, as the chain's leader, announces its price first, and then the retailers determine their profit margins in competition with one another; (2) The seller, as the chain's first leader, makes the decision, and then retailer No. 1 and then retailer No. 2 announce their decision in response to the seller's price; (3) The retailers determine their profit margins simultaneously, and then the seller makes the decision as a follower. (4) Retailer No. 1 is regarded as the market's initial leader. Then retailer No. 2 and the seller make their decisions sequentially, and 5) Retailer No. 1 serves as the leader, with the other seller and retailer making their decisions concurrently. Leng and Parlar (2010) investigated the Stackelberg game in a chain with multiple suppliers and a single follower manufacturer operating under repurchase agreements and sharing lost sales costs. The manufacturer establishes the contract parameters first, and then the suppliers vote in a concurrent game. Cia et al. (2011) presented a SC with a seller and several buyers confronted with the newsboy problem, in which buyers order during the sales season, causing uncertainty. As a leader, one of the buyers may place an order earlier in the season and receive a discount. Two distinct scenarios are considered: (1) the leader buyer has a single ordering opportunity, and (2) the leader buyer has two ordering opportunities. Zhang and Huang (2010) examined a SC involving a manufacturer and a coalition of suppliers. A common platform is used to create a family of products with interchangeable modules. As the customer and chain leader, the manufacturer initially decides on supplier selection and platform configuration. The suppliers then determine the price and quantity of the order in order to maximize the coalition's overall profit.

Liu et al. (2010) evaluated a SC with a manufacturer who distributes its products to the market via two online retailers. The level of access to demand information varies between the two sales channels, and the game is analyzed using contracts in both centralized and decentralized situations. The findings indicate that when uncertainty is high, the manufacturer prefers a basket of contracts, whereas when uncertainty is low, he selects only one contract. Farahani et al. (2014) analyzed over 200 papers and classified them according to the type of competitive SCN design, solution methods, models, and applications. This article establishes a sound foundation for future research. Pritchard (2007) devised a bi-level algorithm for solving the competing SCN problem, in which two chains compete without the presence of a competitor chain. The proposed algorithm was developed using the Lemke and Howson algorithms as a starting point. They then applied the developed model to a real-world case study and analyzed the data. Saghaeeian and Ramezanian (2018) described a multi-product competitive supply chain network (SCN) organization. They began by expanding a bi-level mathematical model of SC members in this paper. They then transformed the competitive chain model into a one-level mathematical model using the KKT method. Finally, they used a hybrid genetic algorithm to solve the problem.

Rezapour et al. (2015) proposed a closed-loop SCN that is price-demand-dependent. Their role in this network was to help the SCN increase its profits. Their model considered strategic objectives such as facility location, tactical objectives such as optimal goods flow allocation, and operational objectives such as product pricing. Finally, they presented a two-step algorithm for resolving the issue. Amiri et al. (2018) developed a bi-level mathematical model for a competitive SC that takes predictive variables into account. They considered using an iterative search method to address the leader's issue. The numerical results indicated that omitting competition discussions results in a loss of market share and profitability for a new competitor's SC. Hassni (2016) proposed a comprehensive model for developing a SCN with multiple periods, multiple products, and multiple stages of inventory control. In the face of static competition, he considered various marketing techniques and methods during the design process. The purpose of the presented model was to achieve an effective customer response in the presence of existing competitors and a lack of demand-meeting prices. For solving his two-objective model, he used the NSGA II algorithm. He indicated that the proposed model and solution algorithm effectively deal with competitive pressure, most notably through the use of an effective marketing strategy. Nobari et al. (2019) presented a two-objective model for developing a competitive closed-loop SCN for new businesses. In the presented paper, they examined competitiveness in both forward and reversed networks concurrently. In the forward chain, competitors compete on selling prices in order to gain a greater share of the market, whereas in reverse logistics, competitors compete on incentive purchase prices. They solved their problem through multi-objective colonial competition.

Sarkar and Bhadouriya (2020) proposed a centralized model for optimizing SC profits and compared it to a Stackelberg game between retailers and manufacturers. Li et al. (2020) presented a four-stage Stackelberg game model with the objective of determining the optimal information investment strategies. This article discusses a SC that is two-tiered, with one manufacturer investing in energy-saving products (ESPs) and another retailer selling the products and incorporating demand forecasting. Noh et al. (2019) proposed a two-tiered SC model that included a manufacturer and a retailer. Three approaches are proposed for resolving the SC's coordination: retailer leader–manufacturer follower, manufacturer leader–retailer follower, and centralized SC. Tang et al. (2020) used a Stackelberg game framework to demonstrate that by establishing a contract between the leader and follower, a CLSC can achieve the same return as a centrally coordinated channel. Ghomi-Avili et al. (2020) presented a robust bi-level mathematical model for a competitive green SCN that takes inventory and pricing decisions into account. By illustrating competition between the leader and follower chains, the bi-level mathematical model method was used, and the model's ability to deal with uncertainties was also used to analyze disruption risks. Nagurney (2021) develops a framework for SCN game theory that incorporates labor constraints through three distinct methods. Equilibrium status was recalculated in response to various imparity-related issues. A case study was then conducted to examine the relationship between COVID-19 and migrant labor.

Sazvar et al. (2021) proposed a bi-objective programming model for designing a CLPSC that examines expired medication reverse flows. Additionally, they controlled the uncertainty parameters via a scenario-based game theory model. A three-party sustainable supply chain network was proposed by Liu et al. (2021). The model was solved using the Nash equilibrium strategy in conjunction with a novel coordination technique. Mozafari et al. (2021) developed a mathematical model of pricing coordination in a two-echelon supply chain in the presence of uncertainty. They used fuzzy numbers to represent demand and production costs. Boronoos et al. (2021) developed a model for a multi-objective closed-loop green supply chain problem that is uncertain. Simultaneously, they used this model to reduce the costs of the entire supply chain network and greenhouse gas emissions in both forward and reverse supply chains. Due to the fact that transportation and operating costs, as well as triangular fuzzy numbers, are considered indefinitely in this demand model, a robust-fuzzy optimization method is used to control these parameters. Liu et al. (2021) proposed a pricing decision model for an uncertain-demand closed-loop supply chain network. They factored in critical decisions such as supplier selection and product flow optimization into their model. Ziari and Sajadieh (2022) proposed a closed-loop supply chain network model based on the pricing structure of the glass industry. Additionally, they investigated network disruptions in the study network. Keshavarz-Ghorbani and Arshadi Khamseh (2022) proposed a multi-period optimization model for a closed-loop supply chain network, taking into account quality control and pricing.

According to the literature review, various researchers have employed a variety of methods and algorithms to address supply chain network problems under a variety of different assumptions. In the majority of cases, well-known algorithms such as the genetic algorithm (GA) and the ant colony algorithm (ACO) have been used. Each algorithm utilizes a unique set of operators to search the solution space. Recent research has shown an increase in the use of population-based algorithms such as GWO, ALO, and others. Numerous studies have demonstrated that the use of population-based algorithms produces superior results. In this paper, taking advantage of the GA operators' strengths (crossover and mutation) and the ALO's high search speed, the operators of the two algorithms were used to search the problem more efficiently and effectively.

Due to the research gap, the manuscript's contributions are divided into two parts: modeling and solution method.

- A competitive supply chain network model (leader–follower) based on the Stackelberg game was proposed under uncertainty.
- The proposed bi-level model was converted to a one-level model using KKT conditions.
- A fuzzy programming approach is used to control the problem's uncertain parameters.
- A novel hybrid genetic and ant-lion optimization algorithm is designed for the model's solution.

3 Problem definition and mathematical modeling

We examine two competing supply chains, one of which is an incumbent whose location of facilities is critical, and the other of which is a new entrant. Each SC is composed of four echelons: suppliers, manufacturers, distribution centers, and retailers. These echelons collaborate to provide final products to a common market. The network of the SC is depicted in Fig. 1. The entrant SC must make several strategic, tactical, and operational decisions, including determining the locations of suppliers, manufacturers, distribution centers, and retailers, to name a few. At the tactical level, each SC determines how the products will be supplied and distributed to the final customers. They determine how much raw material each supplier should provide to each manufacturer, how many products each manufacturer should produce, and how the DCs and retailers should distribute it. Finally, the operational level decision is about product pricing.

The supply chains compete for customers by offering substitutable products in a common market. We assume the incumbent SC is currently operating in the market and that its facility locations are known. As a result, the incumbent does not face such strategic choices. The incumbent, on the other hand, would make tactical and operational adjustments in response to the entrant. As a result, there is a foresight-based competition between the entrant and incumbent supply chains, which can be modeled as a leader–follower or Stackelberg game. Since the entrant initiates the game, anticipating and incorporating the incumbent's response, he or she is the leader. And the incumbent is a follower because he or she accommodates the entrant's tactical and operational decisions following entry. A leader–follower game can be modeled as a bi-level programming problem, as is frequently done in the relevant literature. As a result, our objective is to develop and solve a bi-level mathematical model of the considered problem.

3.1 Demand function

Demand functions are used to model customer purchasing behavior. There are several different types of demand functions described in the relevant literature, but the linear function is the most frequently used model due to its superior characteristics. Kurata et al. (2007) discuss the advantages of the linear demand function, which include proper tracking, traditional microeconomic analysis, and congruence with actual data. As a result of this advantageous characteristic, we chose to use a linear demand model. Customers are assumed to be price sensitive. As a result, we consider the following price-dependent linear demand function.

$$D^{L}_{mp} = \tilde{a}^{L}_{mp} - b^{L}_{mpp}Pr^{L}_{mp} + d^{F}_{mp}Pr^{F}_{mp} - \sum_{\substack{h \in P \\ h \neq p}} b^{L}_{mhp}Pr^{L}_{mh}, \quad \forall m \in M, p \in P \tag{1}$$

$$D^{F}_{mp} = \tilde{a}^{F}_{mp} - b^{F}_{mpp}Pr^{F}_{mp} + d^{L}_{mp}Pr^{L}_{mp} - \sum_{\substack{h \in P \\ h \neq p}} b^{F}_{mhp}Pr^{F}_{mh}, \quad \forall m \in M, p \in P \tag{2}$$

where the superscripts L and F denote, respectively, the leader and follower. Additionally, the following notations are defined.

$\tilde{a}^{\cdot}_{mp}$	The uncertain potential demand of customer segment m for product p
$b^{\cdot}_{mhp}$	The price sensitivity coefficient of customer segment m. If $h = p$, it is self-price sensitivity, and if $h \neq p$, it is cross-price sensitivity and shows the sensitivity of customer's demand from segment m for product p to the price of product h. The products p and h are complementary and produced by the same SC
$d^{\cdot}_{mp}$	The cross-price sensitivity to the price of the other SC. That is, d^{F}_{mp} shows the sensitivity of customer's demand from segment m for product p of the leader SC to the price of product p of the follower SC. And, d^{L}_{mp} represents a similar concept in the followers' demand model
$Pr^{\cdot}_{mp}$	The price of product p for customer segment m

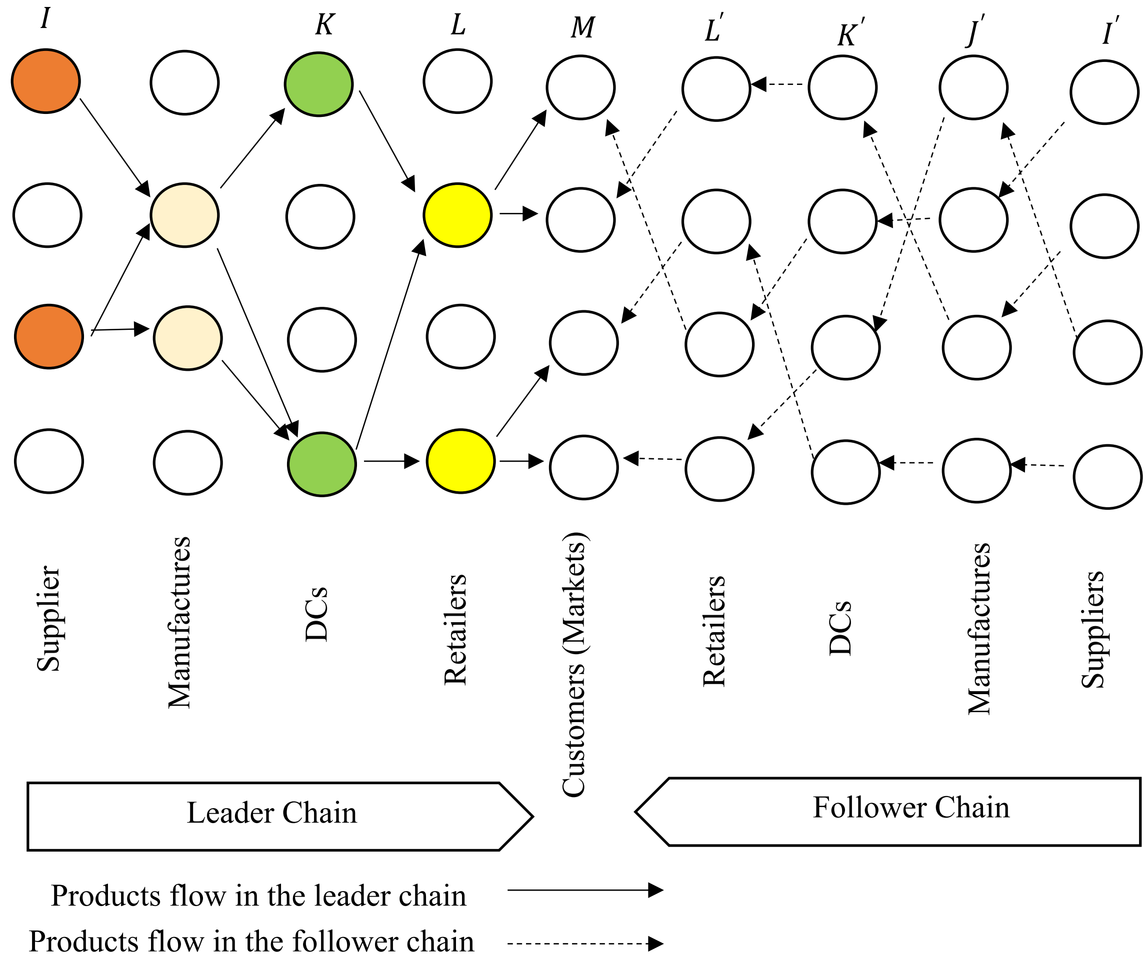

Fig. 1 Proposed supply chain network

The demand for each product from a customer segment m is proportional to its price and the price of its complement products in this demand model. And it is increasing in lockstep with the price of the rival SC's substitutable products.

We permit a product's price to vary across market segments. That is, it is assumed that third-degree discrimination exists in pricing, and chains can charge different prices to different customer segments. The model of supply exceeding demand is prevalent in the pertinent literature.

3.2 Mathematical model

The new SC has been designated as the market leader, whereas the incumbent SC has been designated as the follower. Both SCs are divided into four echelons. Suppliers in the first echelon provide raw materials to manufacturers for the creation of new products. The second echelon is made up of numerous manufacturers who ship their new products to the third echelon's DCs. Finally, retailers in the fourth echelon receive products from DCs and resell them to customers in a variety of markets. While the incumbent SC's location of suppliers, manufacturers, DCs, and retailers is critical, the entrant SC should determine the locations (with pre-determined capacity) of its various members. A horizontal competition between two SCs at the retailer level has been considered. Both of them have the ability to influence the other's demand through pricing decisions. Due to capacity constraints, the chain of followers has already been formed, and it is capacity unrestricted. The network structure of the proposed model is depicted in Fig. 1. The problem has been classified as a bi-level mathematical model due to the Stackelberg game. The upper level presented the problem of the first model, while the lower level defined the problem of the follower. Profit maximization is the primary objective of both chains.

The following are the primary assumptions that guided the development of the mathematical model:

- At both levels, demand for each product in each market is a linear function of self-price, competitor's price, and also the complement-price of their own chain.

- The leader's primary concern has been the need for new facilities.
- No shortage of the leader's chain is permitted.
- Depending on the price and transportation costs, the probable behavior of customers may result in different demands for retailers.
- Each customer can purchase any product in any quantity from any retailer.
- In the third stage, the transport price is equal to the distance between each retailer's various markets for both chains.
- The chain of the follower does not have a budget constraint and is also incapacitated.
- Costs of production and transportation at the upper and lower ends of the spectrum are considered uncertain.

The model is presented using the notations below.

Sets

I	Sets of suppliers in the leader chain $i = \{1, 2, \ldots, I\}$
J	Sets of potential manufactures in the leader chain $j = \{1, 2, \ldots, J\}$
K	Sets of potential DCs in the leader chain $k = \{1, 2, \ldots, K\}$
L	Sets of potential retailers in the leader chain $l = \{1, 2, \ldots, L\}$
M	Sets of fixed markets (Customers) $m = \{1, 2, \ldots, M\}$
I'	Sets of suppliers in the follower chain $i' = \{1, 2, \ldots, I'\}$
J'	Sets of manufactures in the follower chain $j' = \{1, 2, \ldots, J'\}$
K'	Sets of potential DCs in the follower chain $k' = \{1, 2, \ldots, K'\}$
L'	Sets of potential retailers in the follower chain $l' = \{1, 2, \ldots, L'\}$
P	Set of Products $p, h = \{1, 2, \ldots, P\}$
C	Set of raw materials $c = \{1, 2, \ldots, C\}$

Parameters

$FixI_i$	Fixed cost of supplier i in the leader chain
$FixJ_j$	Fixed cost of manufacture j in the leader chain
$FixK_k$	Fixed cost of DC k in the leader chain
$FixL_l$	Fixed cost of retailer l in the leader chain
$\widetilde{TrIJ}^{L}_{ijc}$	The transportation cost of material c between supplier i and manufacture j in the leader chain
$\widetilde{TrJK}^{L}_{jkp}$	The transportation cost of product p between manufacture j and DC k in the leader chain
$\widetilde{TrKL}^{L}_{klp}$	The transportation cost of product p between DC k and retailer l in the leader chain
$\widetilde{TrLM}^{L}_{lmp}$	The transportation cost of product p between retailer l and customer m in the leader chain
$\widetilde{Pc}^{L}_{jp}$	The cost of producing, product p in manufacture j in the leader chain
O_{cp}	The raw material c needed to produce a unit of product p
$CapI_{ic}$	Maximum supplier i capacity of raw material c
$CapJ_{jp}$	Maximum manufacture j capacity of product p
$\mathrm{Cap}K_{kp}$	Maximum DC k capacity of product p
$CapL_{lp}$	Maximum retailer l capacity of product p
$\widetilde{TrIJ}^{F}_{i'j'c}$	The transportation cost of material c between supplier i' and manufacture j' in the follower chain
$\widetilde{TrJK}^{F}_{j'k'p}$	The transportation cost of product p between manufacture j' and DC k' in the follower chain
$\widetilde{TrKL}^{F}_{k'l'p}$	The transportation cost of product p between DC k' and retailer l' in the follower chain
$\widetilde{TrLM}^{F}_{l'mp}$	The transportation cost of product p between retailer l' and customer m in the follower chain
$\widetilde{Pc}^{F}_{j'p}$	The cost of producing, product p in manufacture j' in the follower chain

Decision variables

ZI_i	1 if supplier i is chosen; 0 otherwise
ZJ_j	1 if manufacture j is chosen; 0 otherwise
ZK_k	1 if DC k is chosen; 0 otherwise
ZL_l	1 if retailer l is selected; 0 otherwise
X^{L}_{ijc}	Amount of raw material c transported between supplier i and manufacture j in the leader chain
Y^{L}_{jkp}	Amount of product p transported between manufacture j and DC k in the leader chain
S^{L}_{klp}	Amount of product p transported between DC k and retailer l in the leader chain
U^{L}_{lmp}	Amount of product p transported between retailer l and customer m in the leader chain
$X^{F}_{i'j'c}$	Amount of raw material c transported between supplier i' and manufacture j' in the follower chain
$Y^{F}_{j'k'p}$	Amount of product p transported between manufacture j' and DC k' in the follower chain
$S^{F}_{k'l'p}$	Amount of product p transported between DC k' and retailer l' in the follower chain
$U^{F}_{l'mp}$	Amount of product p transported between retailer l' and customer m in the follower chain
Pr^{L}_{mp}	The price of product p for customer m in the leader chain
Pr^{F}_{mp}	The price of product p for customer m in the follower chain

The bi-level mathematical model of the proposed problem is introduced as below.

3.3 The upper level (leader's model)

$$\begin{aligned}\max\ F_L = &\sum_{l\in L}\sum_{m\in M}\sum_{p\in P} Pr^L_{mp}U^L_{lmp} - \sum_{i\in I}\sum_{j\in J}\sum_{c\in C}\widetilde{TrIJ}^L_{ijc}X^L_{ijc}\\ &-\sum_{j\in J}\sum_{k\in K}\sum_{p\in P}\widetilde{TrJK}^L_{jkp}Y^L_{jkp}\\ &-\sum_{j\in J}\sum_{k\in K}\sum_{p\in P}\widetilde{Pc}^L_{jp}Y^L_{jkp} - \sum_{k\in K}\sum_{l\in L}\sum_{p\in P}\widetilde{TrKL}^L_{klp}S^L_{klp}\\ &-\sum_{l\in L}\sum_{m\in M}\sum_{p\in P}\widetilde{TrLM}^L_{lmp}U^L_{lmp}\\ &-\sum_{i\in I}FixI_iZI_i - \sum_{i\in I}FixJ_jZJ_j - \sum_{k\in K}FixK_kZK_k\\ &-\sum_{l\in L}FixL_lZL_l\end{aligned} \tag{3}$$

s.t. :

$$D^L_{mp} = \tilde{a}^L_{mp} - b^L_{mpp}Pr^L_{mp} + d^F_{mp}Pr^F_{mp} - \sum_{\substack{h\in P\\ h\neq p}} b^L_{mhp}Pr^L_{mh},\quad \forall m\in M, p\in P \tag{4}$$

$$\sum_{l\in L} U^L_{lmp} = D^L_{mp},\quad \forall m\in M, p\in P \tag{5}$$

$$\sum_{m\in M} U^L_{lmp} \le \sum_{k\in K} S^L_{klp},\quad \forall l\in L, p\in P \tag{6}$$

$$\sum_{l\in L} S^L_{klp} \le \sum_{j\in J} Y^L_{jkp},\quad \forall k\in K, p\in P \tag{7}$$

$$\sum_{k\in K}\sum_{p\in P} O_{cp}Y^L_{jkp} \le \sum_{i\in I} X^L_{ijc},\quad \forall j\in J, c\in C \tag{8}$$

$$\sum_{m\in M} U^L_{lmp} \le CapL_{lp}ZL_l,\quad \forall l\in L, p\in P \tag{9}$$

$$\sum_{l\in L} S^L_{klp} \le CapK_{kp}ZK_k,\quad \forall k\in K, p\in P \tag{10}$$

$$\sum_{k\in K} Y^L_{jkp} \le CapJ_{jp}ZJ_j,\quad \forall j\in J, p\in P \tag{11}$$

$$\sum_{j\in J} X^L_{ijc} \le CapI_{ic}ZI_i,\quad \forall i\in I, c\in C \tag{12}$$

$$ZI_i, ZJ_j, ZK_k, ZL_l \in \{0,1\} \tag{13}$$

$$X^L_{ijc}, Y^L_{jkp}, S^L_{klp}, U^L_{lmp}, Pr^L_{mp} \ge 0. \tag{14}$$

3.4 The lower level (follower's model)

$$\begin{aligned}maxF_F = &\sum_{l'\in L'}\sum_{m\in M}\sum_{p\in P} Pr^F_{mp}U^F_{l'mp} - \sum_{i'\in I'}\sum_{j'\in J'}\sum_{c\in C}\widetilde{TrIJ}^F_{i'j'c}X^F_{i'i'c}\\ &-\sum_{j'\in J'}\sum_{k'\in K'}\sum_{p\in P}\widetilde{TrJK}^F_{j'k'p}Y^F_{j'k'p}\\ &-\sum_{j'\in J'}\sum_{k'\in K'}\sum_{p\in P}\widetilde{Pc}^F_{j'p}Y^F_{j'k'p} - \sum_{k'\in K'}\sum_{l'\in L'}\sum_{p\in P}\widetilde{TrKL}^F_{k'l'p}S^F_{k'l'p}\\ &-\sum_{l'\in L'}\sum_{m\in M}\sum_{p\in P}\widetilde{TrLM}^F_{l'mp}U^F_{l'mp}\end{aligned} \tag{15}$$

$s.t.:$

$$D^F_{mp} = \tilde{a}^F_{mp} - b^F_{mpp}Pr^F_{mp} + d^L_{mp}Pr^L_{mp} - \sum_{\substack{h\in P\\ h\neq p}} b^F_{mhp}Pr^F_{mh},\quad \forall m\in M, p\in P \tag{16}$$

$$\sum_{l'\in L'} U^F_{l'mp} = D^F_{mp},\quad \forall m\in M, p\in P \tag{17}$$

$$\sum_{m\in M} U^F_{l'mp} \le \sum_{k'\in K'} S^F_{k'l'p},\quad \forall l'\in L', p\in P \tag{18}$$

$$\sum_{l'\in L'} S^F_{k'l'p} \le \sum_{j'\in J'} Y^F_{j'k'p},\quad \forall k'\in K', p\in P \tag{19}$$

$$\sum_{k'\in K'}\sum_{p\in P} O_{cp}Y^F_{j'k'p} \le \sum_{i'\in I'} X^F_{i'j'c},\quad \forall j'\in J', c\in C \tag{20}$$

$$D^F_{mp} + D^L_{mp} \le \tilde{a}^F_{mp} + \tilde{a}^L_{mp},\quad \forall m\in M, p\in P \tag{21}$$

$$X^F_{i'j'c}, Y^F_{j'k'p}, S^F_{k'l'p}, U^F_{l'mp}, Pr^F_{mp} \ge 0. \tag{22}$$

The objective function (3) seeks to maximize the profit of the leader. Constraint (4) depicts the leader's demand function. Constraints (5)–(8) illustrate the volume of raw materials and products transported between each of the two leadership chain facilities. Constraints (9)–(12) relate to the capacity of network facilities in the leader chain. Constraints (13) and (14) define the range of decision variables in the leader chain.

The objective function (15) seeks to maximize the profit of the follower. Constraint (16) depicts the follower chain's demand function. Constraints (17)–(20) indicate the volume of material or products transported between each of the two follower chain facilities. Constraints (9)–(12) are pertinent to the network's facilities' valence in the leader chain. Constraints (13) and (14) define the range of decision variables in the leader chain. Restriction (21), on the other hand, regulates the demand for leader and follower chains. Therefore, they cannot exceed the potential demand. Restriction (22) defines the leader chain's positive decision variables.

3.5 KKT conditions

In this section, we have introduced the Karush–Kuhn–Tucker (KKT) conditions for the bi-level mathematical model. With regard to the KKT conditions for a bi-level mathematical model, the primary necessary condition for the lower-level problem is that its constraints are convex.

Due to KKT conditions, the convexity of its restriction is critical for the lower-level problem and the concavity of its objective function in a bi-level mathematical model. By incorporating the follower's KKT constraints at the upper level, the optimal strategy of the follower is guaranteed if these conditions are met.

The following is a typical bi-level mathematical model (Gümüş and Floudas 2005).

$$\begin{aligned}
&\max_u f_l(u,w)\\
&\text{s.t.}\\
&H(u,w)=0\\
&\max_w f_f(u,w)\\
&\text{s.t.}:\\
&g_i(u,w)\le 0,\quad \forall i\\
&h_j(i,w)=0,\quad \forall j\\
&u,w\ge
\end{aligned}\tag{23}$$

The above bi-level mathematical model is transformed into the following one-level mathematical model using the KKT conditions (Mokhlesian and Zegordi 2014).

$$\begin{aligned}
&\max_u f_l(u,w)\\
&\text{s.t.}:\\
&G(u,w)\le 0\\
&H(u,w)=0\\
&\nabla f_{f_{w*}}(u,w^*)=0,\quad \forall i\\
&t_i g_i(u,w^*)=0,\quad \forall i\\
&g_i(u,w)\le 0,\quad \forall i\\
&h_j(u,w)=0,\quad \forall j\\
&u,w\ge 0\\
&t_i\ge 0,\quad \forall i
\end{aligned}\tag{24}$$

where u_i denotes the number of dual variables, λ_i denotes the Lagrangian multipliers, and (u,w) denotes the decision variables. Equation (24) satisfies the optimal conditions of the lower-level problem or of the model's followers. For the leader's problem, the Nash equilibrium tactics are obtained by assuming that the follower employs the optimal tactics. Using the KKT conditions, we can convert the bi-level model to a single-level model. As a result, we can be confident that the lower-level optimum solution is global in nature, as defined by the convex constraints and concave objective function. The converted KKT one-level mathematical model is shown below.

$$\begin{aligned}
maxF_L=&\sum_{l\in L}\sum_{m\in M}\sum_{p\in P}Pr^L_{mp}U^L_{lmp}-\sum_{i\in I}\sum_{j\in J}\sum_{c\in C}\widetilde{TrIJ}^L_{ijc}X^L_{ijc}\\
&-\sum_{j\in J}\sum_{k\in K}\sum_{p\in P}\widetilde{TrJK}^L_{jkp}Y^L_{jkp}\\
&-\sum_{j\in J}\sum_{k\in K}\sum_{p\in P}\widetilde{Pc}^L_{jp}Y^L_{jkp}-\sum_{k\in K}\sum_{l\in L}\sum_{p\in P}\widetilde{TrKL}^L_{klp}S^L_{klp}\\
&-\sum_{l\in L}\sum_{m\in M}\sum_{p\in P}\widetilde{TrLM}^L_{lmp}U^L_{lmp}\\
&-\sum_{i\in I}FixI_iZI_i-\sum_{i\in I}FixJ_jZJ_j-\sum_{k\in K}FixK_kZK_k\\
&-\sum_{l\in L}FixL_lZL_l
\end{aligned}\tag{25}$$

s.t. :

$$\sum_{l\in L}U^L_{lmp}=\tilde{a}^L_{mp}-b^L_{mpp}Pr^L_{mp}+d^F_{mp}Pr^F_{mp}-\sum_{\substack{h\in P\\ h\neq p}}b^L_{mhp}Pr^L_{mh},\quad \forall m\in M,p\in P\tag{26}$$

$$\sum_{m\in M}U^L_{lmp}\le\sum_{k\in K}S^L_{klp},\quad \forall l\in L,p\in P\tag{27}$$

$$\sum_{l\in L}S^L_{klp}\le\sum_{j\in J}Y^L_{jkp},\quad \forall k\in K,p\in P\tag{28}$$

$$\sum_{k\in K}\sum_{p\in P}O_{cp}Y^L_{jkp}\le\sum_{i\in I}X^L_{ijc},\quad \forall j\in J,c\in C\tag{29}$$

$$\sum_{m\in M}U^L_{lmp}\le CapL_{lp}ZL_l,\quad \forall l\in L,p\in P\tag{30}$$

$$\sum_{l\in L}S^L_{klp}\le CapK_{kp}ZK_k,\quad \forall k\in K,p\in P\tag{31}$$

$$\sum_{k\in K}Y^L_{jkp}\le CapJ_{jp}ZJ_j,\quad \forall j\in J,p\in P\tag{32}$$

$$\sum_{j\in J}X^L_{ijc}\le CapI_{ic}ZI_i,\quad \forall i\in I,c\in C\tag{33}$$

$$\sum_{l'\in L'}U^F_{l'mp}=\tilde{a}^F_{mp}-b^F_{mpp}Pr^F_{mp}+d^L_{mp}Pr^L_{mp}-\sum_{\substack{h\in P\\ h\neq p}}b^F_{mhp}Pr^F_{mh},\quad \forall m\in M,p\in P\tag{34}$$

$$\sum_{l'\in L'}U^F_{l'mp}=D^F_{mp},\quad \forall m\in M,p\in P\tag{35}$$

$$\sum_{m\in M} U^F_{l'mp} \le \sum_{k'\in K'} S^F_{k'l'p}, \quad \forall l' \in L', p \in P \tag{36}$$

$$\sum_{l'\in L'} S^F_{k'l'p} \le \sum_{j'\in J'} Y^F_{j'k'p}, \quad \forall k' \in K', p \in P \tag{37}$$

$$\left(\left(\tilde{a}^F_{mp} - b^F_{mpp}Pr^F_{mp} + d^L_{mp}Pr^L_{mp} - \sum_{\substack{h \in P \\ h \ne p}} b^F_{mhp}Pr^F_{mh}\right) + \left(\tilde{a}^L_{mp} - b^L_{mpp}Pr^L_{mp} + d^L_{mp}Pr^L_{mp} - \sum_{\substack{h \in P \\ h \ne p}} b^L_{mhp}Pr^L_{mh}\right)\right) \le \left(\tilde{a}^F_{mp} + \tilde{a}^L_{mp}\right), \quad \forall m \in M, p \in P \tag{38}$$

$$\sum_{m\in M}\sum_{p\in P}\left(\begin{array}{c} \tilde{a}^F_{mp} - b^F_{mpp}Pr^F_{mp} + d^L_{mp}Pr^L_{mp} - \sum_{\substack{h \in P \\ h \ne p}} b^F_{mhp}Pr^F_{mh} - \lambda^1_{mpp}b^F_{mpp} \\ - \sum_{\substack{h \in P \\ h \ne p}} b^F_{mhp}\lambda^1_{mhp} + u^4_{mpp}b^F_{mpp} + \sum_{\substack{h \in P \\ h \ne p}} b^F_{mhp}u^4_{mhp} \end{array}\right) = 0 \tag{39}$$

$$-\sum_{i'\in I'}\sum_{j'\in J'}\sum_{c\in C} \widetilde{TrIJ}^F_{i'j'c} + |I'|\sum_{j'\in J'}\sum_{c\in C} u^1_{j'c} = 0 \tag{40}$$

$$-\sum_{j'\in J'}\sum_{k'\in K'}\sum_{p\in P} \widetilde{TrJK}^F_{j'k'p} - |K'|\sum_{j'\in J'}\sum_{p\in P} \widetilde{Pc}^F_{j'p} - |K'|\sum_{j'\in J'}\sum_{c\in C}\sum_{p\in P} u^1_{j'p}O_{cp} + |J'|\sum_{k'\in K'}\sum_{p\in P} u^2_{k'p} = 0 \tag{41}$$

$$-\sum_{k'\in K'}\sum_{l'\in L'}\sum_{p\in P} \widetilde{TrKL}^F_{k'l'p} - |L'|\sum_{k'\in K'}\sum_{p\in P} u^2_{k'p} + |K'|\sum_{l'\in L'}\sum_{p\in P} u^3_{l'p} = 0 \tag{42}$$

$$-\sum_{l'\in L'}\sum_{m\in M}\sum_{p\in P} \widetilde{TrLM}^F_{l'mp} - |M|\sum_{l'\in L'}\sum_{p\in P} u^3_{l'p} - |L'|\sum_{m\in M}\sum_{p\in P} \lambda^1_{mpp} = 0 \tag{43}$$

$$u^1_{j'c}\left(\sum_{k'\in K'}\sum_{p\in P} O_{cp}Y^F_{j'k'p} - \sum_{i'\in I'} X^F_{i'j'c}\right) = 0, \quad \forall j' \in J', c \in C \tag{44}$$

$$u^2_{k'p}\left(\sum_{l'\in L'} S^F_{k'l'p} - \sum_{j'\in J'} Y^F_{j'k'p}\right) = 0, \quad \forall k' \in K', p \in P \tag{45}$$

$$u^3_{l'p}\left(\sum_{m\in M} U^F_{l'mp} - \sum_{k'\in K'} S^F_{k'l'p}\right) = 0, \quad \forall l' \in L', p \in P \tag{46}$$

$$\lambda^1_{mpp}\left(\sum_{l'\in L'} U^F_{l'mp} - \tilde{a}^F_{mp} + b^F_{mpp}Pr^F_{mp} - d^L_{mp}Pr^L_{mp} + \sum_{\substack{h \in P \\ h \ne p}} b^F_{mhp}Pr^F_{mh}\right) = 0, \quad \forall m \in M, p \in P \tag{47}$$

$$u^4_{mpp}\left(\begin{array}{c} \left(\tilde{a}^F_{mp} - b^F_{mpp}Pr^F_{mp} + d^L_{mp}Pr^L_{mp} - \sum_{\substack{h \in P \\ h \ne p}} b^F_{mhp}Pr^F_{mh}\right) \\ + \left(\tilde{a}^L_{mp} - b^L_{mpp}Pr^L_{mp} + d^L_{mp}Pr^L_{mp} - \sum_{\substack{h \in P \\ h \ne p}} b^L_{mhp}Pr^L_{mh}\right) \\ -\left(\tilde{a}^F_{mp} + \tilde{a}^L_{mp}\right) \end{array}\right) = 0, \quad \forall m \in M, p \in P \tag{48}$$

$$\tilde{a}^F_{mp} - b^F_{mpp}Pr^F_{mp} + d^L_{mp}Pr^L_{mp} - \sum_{\substack{h \in P \\ h \ne p}} b^F_{mhp}Pr^F_{mh} \ge 0, \quad \forall m \in M, p \in P \tag{49}$$

$$\tilde{a}^L_{mp} - b^L_{mpp}Pr^L_{mp} + d^L_{mp}Pr^L_{mp} - \sum_{\substack{h \in P \\ h \ne p}} b^L_{mhp}Pr^L_{mh} \ge 0, \quad \forall m \in M, p \in P \tag{50}$$

$$ZI_i, ZJ_j, ZK_k, ZL_l \in \{0, 1\} \tag{51}$$

$$X^L_{ijc}, Y^L_{jkp}, S^L_{klp}, U^L_{lmp}, Pr^L_{mp}, X^F_{i'j'c}, Y^F_{j'k'p}, S^F_{k'l'p}, U^F_{l'mp}, Pr^F_{mp}, \ge 0. \tag{52}$$

3.6 Fuzzy programming model

Consider the following linear mathematical programming model with fuzzy parameters (Yildizbaşi et al. 2018):

$$\begin{aligned} &\operatorname{Max} Z=\tilde{c}^t x \\ &\qquad \text{s.t. :} \\ &\qquad x \in N(\tilde{A}, \tilde{B})=\{x \in R^n \mid \tilde{a}_i x \geq \tilde{b}_i, \quad i \in m \quad x \geq 0\} \end{aligned} \tag{53}$$

where $\widetilde{c}=(\widetilde{c}_1, \widetilde{c}_2, \ldots, \widetilde{c}_n), A=[\widetilde{a}_{ij}]_{m \times n}, \widetilde{b}=\left(\widetilde{b}_1, \widetilde{b}_2, \ldots, \widetilde{b}_n\right)^t$ are the fuzzy parameters used in the problem's objective function, the vector coefficient, and the right-side parameter of the constraints? The probability distribution function of fuzzy parameters is assumed based on the properties of fuzzy numbers. Finally $x=(x_1, x_2, \ldots, x_n)$ represents the decision vector. For the feasibility and optimization of the problem presented in the above model, it is necessary to control the uncertain parameters given in the objective function and constraints. Hence, assuming parameter α as the minimum feasibility of constraints, the controlled model is as follows:

$$\begin{aligned} &\operatorname{Max} Z=\mathrm{EV}(\tilde{c}) x \\ &\text{s.t. :} \\ &\left[(1-\alpha) E_2^{a_i}+\alpha E_1^{a_i}\right] x \geq(1-\alpha) E_1^{b_i}+\alpha E_2^{b_i}, \\ &\quad i \in m \quad x \geq 0, \quad \alpha \in[0,1]. \end{aligned} \tag{54}$$

$\mathrm{EV}(\tilde{c})$ is the anticipated value of the fuzzy membership function used in the objective function (OBFV) of the model, which is calculated as follows:

$$\mathrm{EV}(\tilde{c})=\frac{E_1^c+E_2^c}{2}. \tag{55}$$

In this paper, the fuzzy parameters are intended as triangular fuzzy, as illustrated in Fig. 2. Figure 2 indicates the possibilistic distribution of the fuzzy parameter $\widetilde{C}=(C^1, C^2, C^3)$. C^2, C^1, and C^3 represent the optimistic, probable, and pessimistic values of the fuzzy number $\widetilde{C}$, respectively, which are characterized by the decision-maker.

Thus, the expected value (the anticipated value of the fuzzy parameter of the OBFV) can be calculated in the following manner:

$$\mathrm{EI}(\widetilde{c})=\left[E_1^c, E_2^c\right]=\left[\frac{c^1+c^2}{2}, \frac{c^2+c^3}{2}\right]. \tag{56}$$

As mentioned previously, uncertain parameters include the potential demand, upper and lower-level transport costs, as well as upper and lower-level production costs. As a result, the stated uncertain parameters are controlled using a triangular fuzzy programming method.

Parameter	Optimistic	Probable	Pessimistic
$\widetilde{a}_{mp}^F$	$a1_{mp}^F$	$a2_{mp}^F$	$a3_{mp}^F$
$\widetilde{a}_{mp}^L$	$a1_{mp}^L$	$a2_{mp}^L$	$a3_{mp}^L$
$\widetilde{TrIJ}_{ijc}^L$	$TrIJ1_{ijc}^L$	$TrIJ2_{ijc}^L$	$TrIJ3_{ijc}^L$
$\widetilde{TrJK}_{jkp}^L$	$TrJK1_{jkp}^L$	$TrJK2_{jkp}^L$	$TrJk3_{jkp}^L$
$\widetilde{TrKL}_{klp}^L$	$TrKL1_{klp}^L$	$TrKL2_{klp}^L$	$TrKL3_{klp}^L$
$\widetilde{TrLM}_{lmp}^L$	$TrLM1_{lmp}^L$	$TrLM2_{lmp}^L$	$TrLM3_{lmp}^L$
$\widetilde{Pc}_{jp}^L$	$Pc1_{jp}^L$	$Pc2_{jp}^L$	$Pc3_{jp}^L$
$\widetilde{TrIJ}_{i'j'c}^F$	$TrIJ1_{i'j'c}^F$	$TrIJ2_{i'j'c}^F$	$TrIJ3_{i'j'c}^F$
$\widetilde{TrJK}_{j'k'p}^F$	$TrJK1_{j'k'p}^F$	$TrJK2_{j'k'p}^F$	$TrJK3_{j'k'p}^F$
$\widetilde{TrKL}_{k'l'p}^F$	$TtKL1_{k'l'p}^F$	$TtKL2_{k'l'p}^F$	$TtKL3_{k'l'p}^F$
$\widetilde{TrLM}_{l'mp}^F$	$TrLM1_{l'mp}^F$	$TrLM2_{l'mp}^F$	$TrLM3_{l'mp}^F$
$\widetilde{Pc}_{j'p}^F$	$Pc1_{j'p}^F$	$Pc2_{j'p}^F$	$Pc3_{j'p}^F$

As a result of the expressed relationships, we can write the fuzzy programming model as follows:

$$\begin{aligned} \max[F_L]= & \sum_{l \in L} \sum_{m \in M} \sum_{p \in P} Pr_{mp}^L U_{lmp}^L \\ & -\sum_{i \in I} \sum_{j \in J} \sum_{c \in C}\left(\frac{TrIJ1_{ijc}^L+2 TrIJ2_{ijc}^L+TrIJ3_{ijc}^L}{4}\right) X_{ijc}^L \\ & -\sum_{j \in J} \sum_{k \in K} \sum_{p \in P}\left(\frac{TrJK1_{jkp}^L+2 TrJK1_{jkp}^L+TrJK3_{jkp}^L}{4}\right) Y_{jkp}^L \\ & -\sum_{j \in J} \sum_{k \in K} \sum_{p \in P}\left(\frac{Pc1_{jp}^L+2 Pc2_{jp}^L+Pc3_{jp}^L}{4}\right) Y_{jkp}^L \\ & -\sum_{k \in K} \sum_{l \in L} \sum_{p \in P}\left(\frac{TrKL1_{klp}^L+2 TrKL1_{klp}^L+TrKL3_{klp}^L}{4}\right) S_{klp}^L \\ & -\sum_{l \in L} \sum_{m \in M} \sum_{p \in P}\left(\frac{TrLM1_{jkp}^L+2 TrLM1_{jkp}^L+TrLM3_{jkp}^L}{4}\right) U_{lmp}^L \\ & -\sum_{i \in I} FixI_i ZI_i-\sum_{i \in I} FixJ_j ZJ_j-\sum_{k \in K} FixK_k ZK_k \\ & -\sum_{l \in L} FixL_l ZL_l \end{aligned} \tag{57}$$

$s.t.:$

$$\sum_{l\in L} U^L_{lmp} = \begin{pmatrix} \alpha\left(\dfrac{a2^L_{mp}+a3^L_{mp}}{2}\right)+ \\ (1-\alpha)\left(\dfrac{a2^L_{mp}+a1^L_{mp}}{2}\right)\end{pmatrix} - b^L_{mpp}\overset{L}{\underset{mp}{\Pr}} + d^F_{mp}\overset{F}{\underset{mp}{\Pr}} - \sum_{\substack{h\in P\\ h\neq p}} b^L_{mhp}\overset{L}{\underset{mh}{\Pr}}, \quad \forall m\in M, p\in P \tag{58}$$

$$\sum_{l'\in L'} U^F_{l'mp} = \begin{pmatrix} \beta\left(\dfrac{a2^F_{mp}+a3^F_{mp}}{2}\right)+ \\ (1-\beta)\left(\dfrac{a2^F_{mp}+a1^F_{mp}}{2}\right)\end{pmatrix} - b^F_{mpp}\overset{F}{\underset{mp}{\Pr}} + d^L_{mp}\overset{L}{\underset{mp}{\Pr}} - \sum_{\substack{h\in P\\ h\neq p}} b^F_{mhp}\overset{F}{\underset{mh}{\Pr}}, \tag{59}$$

$\forall m\in M, p\in P$

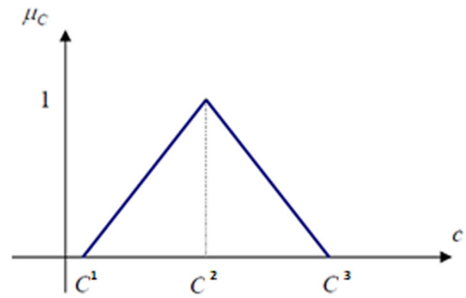

Fig. 2 The possibilistic distribution of the fuzzy parameter C

$$\sum_{m\in M}\sum_{p\in P}\left(\begin{array}{c} \begin{pmatrix} \beta\left(\dfrac{a2^F_{mp}+a3^F_{mp}}{2}\right)+ \\ (1-\beta)\left(\dfrac{a2^F_{mp}+a1^F_{mp}}{2}\right)\end{pmatrix} - b^F_{mpp}Pr^F_{mp} + d^L_{mp}Pr^L_{mp} - \\ \sum_{\substack{h\in P\\ h\neq p}} b^F_{mhp}Pr^F_{mh} - \lambda^1_{mpp}b^F_{mpp} \\ -\sum_{\substack{h\in P\\ h\neq p}} b^F_{mhp}\lambda^1_{mhp} + u^4_{mpp}b^F_{mpp} + \sum_{\substack{h\in P\\ h\neq p}} b^F_{mhp}u^4_{mhp} \end{array}\right) \tag{61}$$

$$\begin{array}{l}\left(\begin{array}{c}\left(\begin{pmatrix} \beta\left(\dfrac{a2^F_{mp}+a3^F_{mp}}{2}\right)+ \\ (1-\beta)\left(\dfrac{a2^F_{mp}+a1^F_{mp}}{2}\right)\end{pmatrix} - b^F_{mpp}Pr^F_{mp} + d^L_{mp}Pr^L_{mp} - \sum_{\substack{h\in P\\ h\neq p}} b^F_{mhp}Pr^F_{mh}\right)+ \\ \left(\begin{pmatrix} \alpha\left(\dfrac{a2^L_{mp}+a3^L_{mp}}{2}\right)+ \\ (1-\alpha)\left(\dfrac{a2^L_{mp}+a1^L_{mp}}{2}\right)\end{pmatrix} - b^L_{mpp}Pr^L_{mp} + d^L_{mp}Pr^L_{mp} - \sum_{\substack{h\in P\\ h\neq p}} b^L_{mhp}Pr^L_{mh}\right)\end{array}\right) \\ \leq \left(\begin{pmatrix} \beta\left(\dfrac{a2^F_{mp}+a3^F_{mp}}{2}\right)+ \\ (1-\beta)\left(\dfrac{a2^F_{mp}+a1^F_{mp}}{2}\right)\end{pmatrix} + \begin{pmatrix} \alpha\left(\dfrac{a2^L_{mp}+a3^L_{mp}}{2}\right)+ \\ (1-\alpha)\left(\dfrac{a2^L_{mp}+a1^L_{mp}}{2}\right)\end{pmatrix}\right), \quad \forall m\in M, p\in P\end{array} \tag{60}$$

$$
-\sum_{i'\in I'}\sum_{j'\in J'}\sum_{c\in C}\left(\frac{TrIJ1^F_{i'j'c}+2TrIJ2^F_{i'j'c}+TrIJ3^F_{i'j'c}}{4}\right)+|I'|\sum_{j'\in J'}\sum_{c\in C}u^1_{j'c}=0 \tag{62}
$$

$$
\begin{aligned}
&-\sum_{j'\in J'}\sum_{k'\in K'}\sum_{p\in P}\left(\frac{TrJK1^F_{j'k'p}+2TrJK2^F_{j'k'p}+TrJK3^F_{j'k'p}}{4}\right)\\
&-|K'|\sum_{j'\in J'}\sum_{p\in P}\left(\frac{Pc1^F_{j'p}+2Pc2^F_{j'p}+Pc3^F_{j'p}}{4}\right)\\
&-|K'|\sum_{j'\in J'}\sum_{c\in C}\sum_{p\in P}u^1_{j'p}O_{cp}+|J'|\sum_{k'\in K'}\sum_{p\in P}u^2_{k'p}=0
\end{aligned} \tag{63}
$$

$$
\begin{aligned}
&-\sum_{l'\in L'}\sum_{m\in M}\sum_{p\in P}\left(\frac{TtKL1^F_{k'l'p}+2TtKL2^F_{k'l'p}+TtKL3^F_{k'l'p}}{4}\right)\\
&-|M|\sum_{l'\in L'}\sum_{p\in P}u^3_{l'p}-|L'|\sum_{m\in M}\sum_{p\in P}\lambda^1_{mpp}=0
\end{aligned} \tag{65}
$$

$$
\lambda^1_{mpp}\left(\sum_{l'\in L'}U^F_{l'mp}-\left(\begin{array}{c}\beta\left(\dfrac{a2^F_{mp}+a3^F_{mp}}{2}\right)+\\(1-\beta)\left(\dfrac{a2^F_{mp}+a1^F_{mp}}{2}\right)\end{array}\right)+b^F_{mpp}Pr^F_{mp}-d^L_{mp}Pr^L_{mp}+\sum_{\substack{h\in P\\h\neq p}}b^F_{mhp}Pr^F_{mh}\right)=0,\quad\forall m,p \tag{66}
$$

$$
u^4_{mpp}\left(\begin{array}{l}\left(\left(\begin{array}{c}\beta\left(\dfrac{a2^F_{mp}+a3^F_{mp}}{2}\right)+\\(1-\beta)\left(\dfrac{a2^F_{mp}+a1^F_{mp}}{2}\right)\end{array}\right)-b^F_{mpp}Pr^F_{mp}+d^L_{mp}Pr^L_{mp}-\sum_{\substack{h\in P\\h\neq p}}b^F_{mhp}Pr^F_{mh}\right)\\
+\left(\left(\begin{array}{c}\alpha\left(\dfrac{a2^L_{mp}+a3^L_{mp}}{2}\right)+\\(1-\alpha)\left(\dfrac{a2^L_{mp}+a1^L_{mp}}{2}\right)\end{array}\right)-b^L_{mpp}Pr^L_{mp}+d^L_{mp}Pr^L_{mp}-\sum_{\substack{h\in P\\h\neq p}}b^L_{mhp}Pr^L_{mh}\right)\\
-\left(\left(\begin{array}{c}\beta\left(\dfrac{a2^F_{mp}+a3^F_{mp}}{2}\right)+\\(1-\beta)\left(\dfrac{a2^F_{mp}+a1^F_{mp}}{2}\right)\end{array}\right)+\left(\begin{array}{c}\alpha\left(\dfrac{a2^L_{mp}+a3^L_{mp}}{2}\right)+\\(1-\alpha)\left(\dfrac{a2^L_{mp}+a1^L_{mp}}{2}\right)\end{array}\right)\right)\end{array}\right)=0,\quad\forall m,p \tag{67}
$$

$$
\begin{aligned}
&-\sum_{k'\in K'}\sum_{l'\in L'}\sum_{p\in P}\left(\frac{TtKL1^F_{k'l'p}+2TtKL2^F_{k'l'p}+KL3^F_{k'l'p}}{4}\right)\\
&-|L'|\sum_{k'\in K'}\sum_{p\in P}u^2_{k'p}+|K'|\sum_{l'\in L'}\sum_{p\in P}u^3_{l'p}=0
\end{aligned} \tag{64}
$$

$$
\left(\begin{array}{c}\beta\left(\dfrac{a2^F_{mp}+a3^F_{mp}}{2}\right)+\\(1-\beta)\left(\dfrac{a2^F_{mp}+a1^F_{mp}}{2}\right)\end{array}\right)-b^F_{mpp}Pr^F_{mp}+d^L_{mp}Pr^L_{mp}-\sum_{\substack{h\in P\\h\neq p}}b^F_{mhp}Pr^F_{mh}\geq 0,\quad\forall m,p \tag{68}
$$

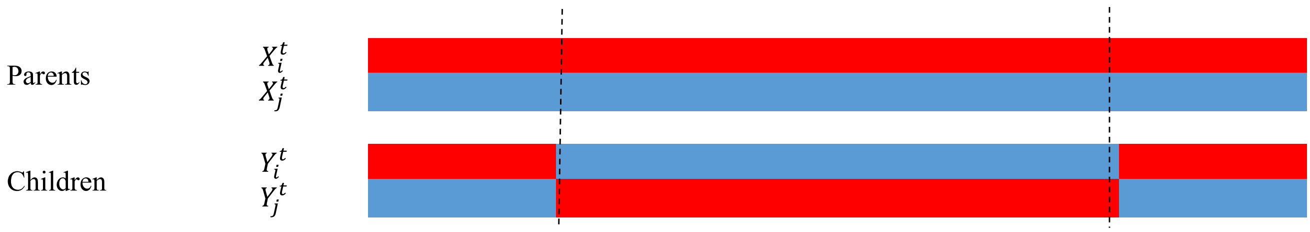

Fig. 3 Two-point crossover operator

Fig. 4 Mutation operator

$$\begin{pmatrix} \alpha\left(\dfrac{a2^L_{mp}+a3^L_{mp}}{2}\right)+ \\ (1-\alpha)\left(\dfrac{a2^L_{mp}+a1^L_{mp}}{2}\right) \end{pmatrix} - b^L_{mpp}Pr^L_{mp} + d^L_{mp}Pr^L_{mp}$$
$$-\sum_{\substack{h\in P\\ h\neq p}} b^L_{mhp}Pr^L_{mh} \geq 0, \quad \forall m,p \tag{69}$$

$$ZI_i, ZJ_j, ZK_k, ZL_l \in \{0,1\} \tag{70}$$

Eqs (27)–(33) Eqs (30)–(37) Eqs (44)–(46) Eqs (51)–(52)

where $u^1_{j'c}, u^2_{k'p}, u^3_{l'p}, u^4_{mpp}$ are dual variables and λ^1_{mpp} is the Lagrangian multiplier.

The proposed leader–follower model produces a MINLP. Numerous studies have established the NP-hardness of the SCN design problem (Jayaraman et al. 2003). The developed model addresses two distinct problems: location and allocation. As a result, this model can be reduced to the facility location problem, which has been shown to be NP-hard (Davis and Ray 1969). As a result, the aforementioned leader–follower SCN problem is introduced in this study as NP-hard. Accurately resolving this problem through precise solutions is time-consuming and frequently impractical. Thus, numerous meta-heuristic algorithms with various representations have been proposed to achieve near-optimal solutions, but they are inefficient. The following section describes the HGALO algorithm.

4 Hybrid genetic ant-lion optimization algorithm

The ant-lion algorithm mimics the hunting mechanism of the ant lion and interacts with the bait, the desired ant, and imitates them all (Mirjalili 2015). As with other population-based algorithms, the ant-lion algorithm approximates optimal solutions to optimization problems by promoting a random set of solutions inspired by the ant-lion interaction. The ant-lion algorithm has two populations: ants and ant lions. This article discusses how to improve the approximate optimal solutions for leader–follower SCN design by utilizing crossover and mutation operators. The ant-lion algorithm's general stages for changing these sets and, finally, for global optimization estimation are as follows:

A. The ant set is initiated using random values, which is the most critical factor in determining the ant-lion algorithm.
B. The value of each ant's fit is determined in each replication using the (OBFV).
C. The ants in the search area are scurrying about the ant lions at random.
D. The crowd of ant lions is never evaluated. The ant lions are supposed to be positioned in the first reps and will move toward the new position of the ants remaining in the repeats; of course, if they improve, they will move toward the new position of the ants remaining in the repeats.
E. An ant is assigned to one ant lion, and its position is revealed as the ant gains fitness.
F. There is an ant lion nearby that, regardless of its distance, has an effect on the ants' movement.
G. If any ant lion is found to be preferable to the selected ant, it will be replaced.

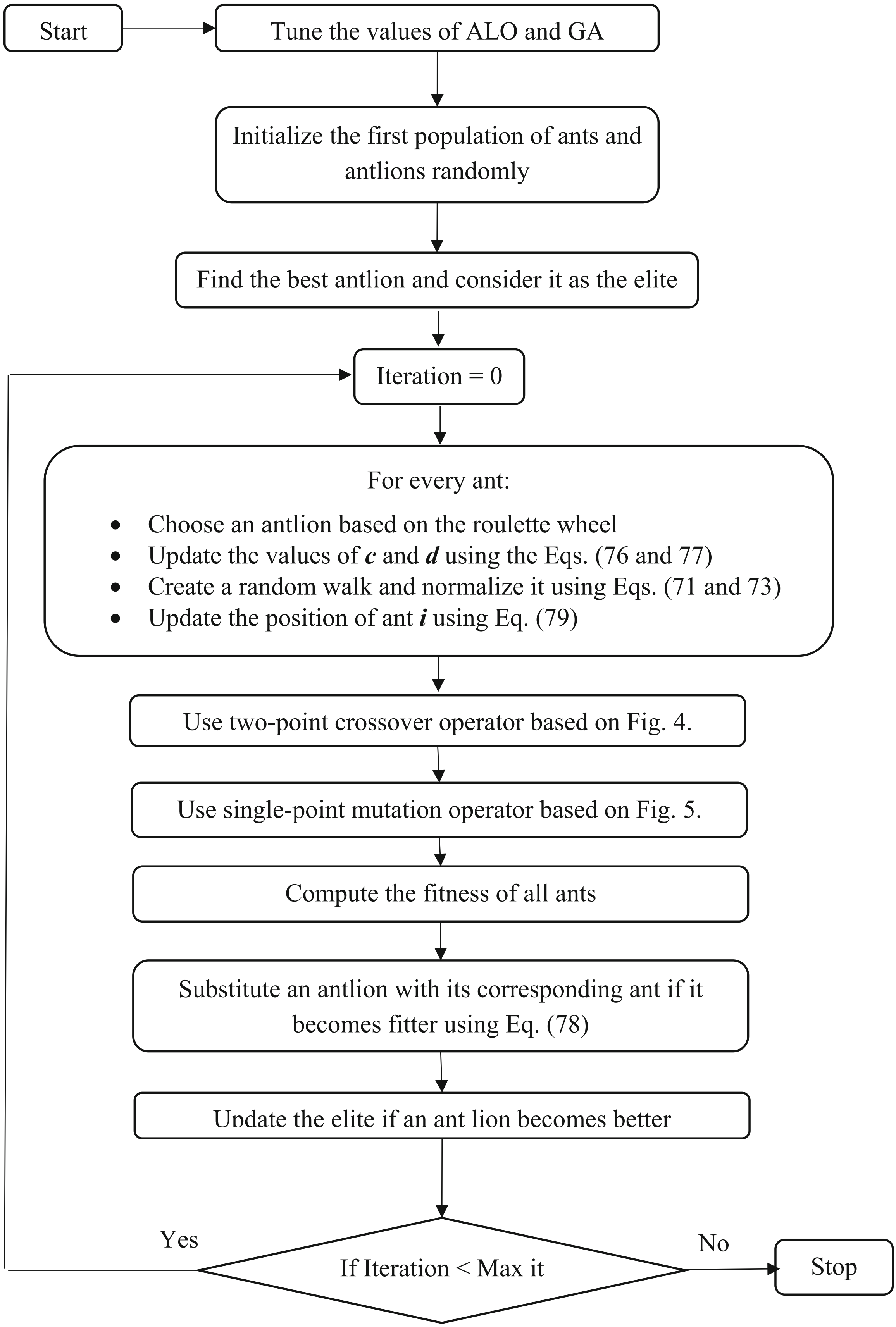

Fig. 5 The flowchart of HGALO

H. The stages (B) to (E) are repeated until the final criterion is deemed satisfactory, and

I. For global optimization, the fitting position and value of the selected ant lion are returned as the most accurate estimate.

Ants' primary role is to inspect the search area. They should proceed randomly through the search area. Ant lions select the best ants and direct them to promising search areas. To solve the problems optimally, the ant-lion algorithm emulates the ants' random steps, immersion in the ant-lion cavity, creation of the cavity, movement of the ant to ant lions, catching the bait, repairing the cavity, and selection of the preferred one. The following par diagrams illustrate the model and programming modules associated with each step. The randomized step used in the ant-lion algorithm to simulate the random steps of an ant is as follows:

$$X(t) = [0, \mathrm{cumsum}(2r(t_1) - 1), \mathrm{cumsum}(2r(t_2) - 1), \ldots, \mathrm{cumsum}(2r(t_n) - 1)] \tag{71}$$

where cumsum denotes the cumulative sum, n denotes the maximum number of repeats, and t denotes the step size of a random step.

$$r(t) = \begin{cases} 1 & \text{if } \mathrm{rand} > 0.5 \\ 0 & \text{if } \mathrm{rand} \le 0.5 \end{cases} \tag{72}$$

t denotes a random step (in this paper, repetition) and rand denotes a random number of births distributed uniformly within the interval [0,1]. To maintain a random step on the search space's boundaries and avoid over-hunting, random steps must be normalized to the following equation.

$$X_i^t = \frac{\left(X_i^t - a_i\right) \times \left(d_i^t - c_i^t\right)}{\left(b_i - a_i\right)} + c_i^t \tag{73}$$

where c_i^t is the least significant variable in repetition t, d_i^t is the maximum variable i in repetition t, a_i is the min of random variable i, and b_i is the max random step in the variable i. Ant-lion algorithm simulates the ants' clogging in the ant-lion hole by changing the ant-lions' random steps. The following equations are presented in this regard:

$$c_i^t = \mathrm{Antlion}_j^t + c^t \tag{74}$$

$$d_i^t = \mathrm{Antlion}_j^t + d^t \tag{75}$$

where c^t is the minimum variables in repetition t, d^t is a vector containing the maximum of all variables in repetition t, c_i^t is the min variables for variable i, d_i^t is max of all the variables for ant i, $\mathrm{Antlion}_j^t$ is the position of the ant lion chosen in repetition t.

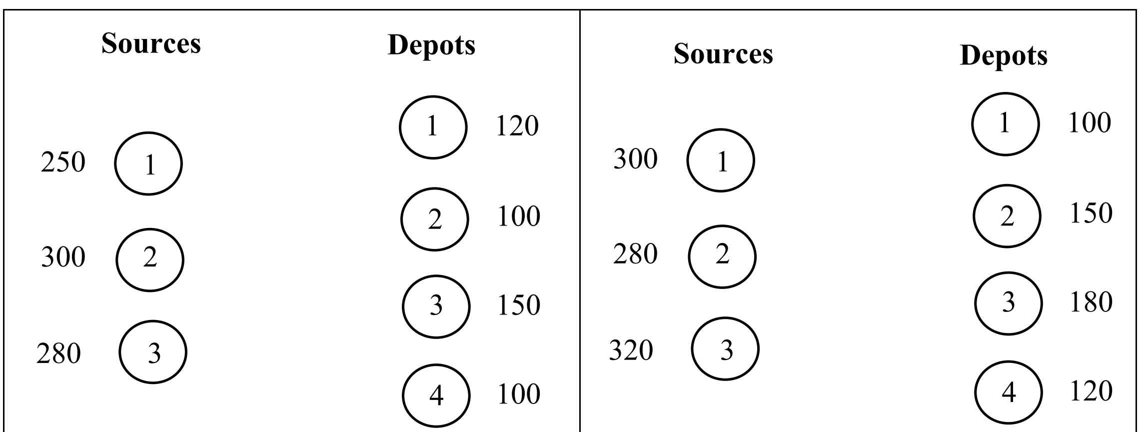

$$\mathit{Transportation\ Cost} = \boldsymbol{Sources}\ \underbrace{\begin{bmatrix} 2 & 5 & 1 & 4 \\ 4 & 3 & 2 & 6 \\ 5 & 2 & 7 & 3 \end{bmatrix}}_{\boldsymbol{Depots}}$$

chromosome $\{(|K| + |J|) * |P|\}$

Nodes	Source-1	Source-2	Source-3	Depot-1	Depot-2	Depot-3	Depot-4
Product 1	2	7	6	1	3	5	4
Product 2	1	5	3	2	6	4	7

Fig. 6 A sample of SCN chromosome

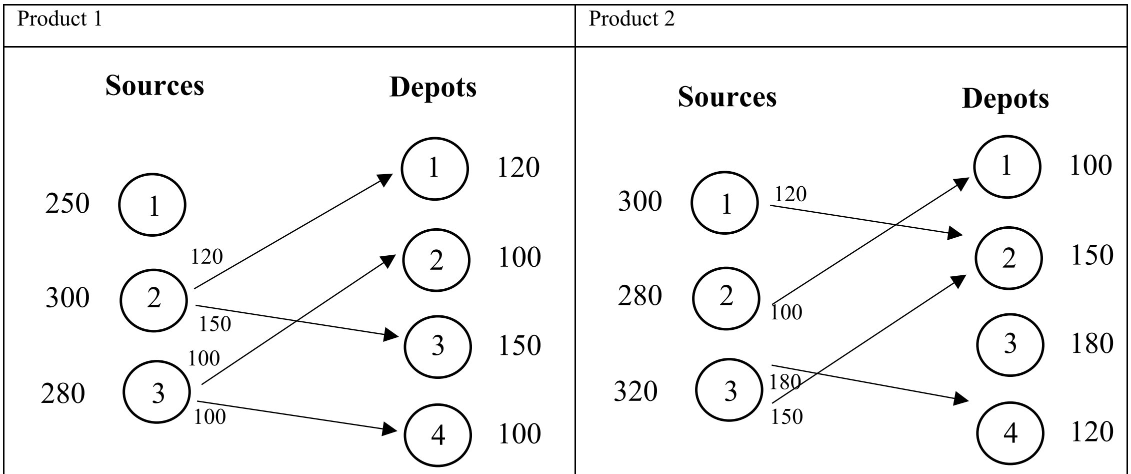

$$\mathit{Transportation\ Cost} = \boldsymbol{Sources}\ \underset{\boldsymbol{Depots}}{\begin{bmatrix} 2 & 5 & 1 & 4 \\ 4 & 3 & 2 & 6 \\ 5 & 2 & 7 & 3 \end{bmatrix}}$$

chromosome $\{(|K| + |J|) * |P|\}$

Nodes	Source-1	Source-2	Source-3	Depot-1	Depot-2	Depot-3	Depot-4
Product 1	0	7	6	1	3	5	4
Product 2	0	5	3	2	6	4	7

Fig. 7 Decoding the sample chromosome

$$c^t = \frac{c^t}{I} \tag{76}$$

$$d^t = \frac{d^t}{I} \tag{77}$$

where I is a ratio, c^t is min of all variables in repetition t, and d^t shows the vector representing the maximum of all the variables in repetition t. In the above equations $I = 1 + 10^w \frac{t}{T}$, in which t is the current repetition, T is the max number of repetitions and w's definition is based on the current replication ($w = 2$ when $t > 0.1T$, $w = 3$ when $t > 0.5T$, $w = 4$ when $t > 0.75T$, $w = 5$ when $t > 0.9T$ and $w = 6$ when $t > 0.95T$). Parameter W in the equation I can be used for adjusting the level of operation accuracy. The 2nd stage up to the last stage of the ant-lion algorithm is to catch the ant and rebuild the pit. The following equation stimulates this process:

$$\text{Antlion}_j^t = \text{Ant}_i^t \quad \text{if} \quad f\left(\text{Ant}_i^t\right) < f\left(\text{Antlion}_j^t\right) \tag{78}$$

where t shows the current repetition, Antlion_j^t indicates the position of the selected ant lion i in repetition t, Ant_i^t indicates position i in repetition t. The last operator in the ant-lion algorithm is the elitism in which the best-fitted formed ant lion is stored during the optimization. This is the single ant lion which can affect all ants. This means moving the selected ant lion (randomly selected using a Rolette wheel) to the ant lion. The equation follows both of them:

$$\text{Ant}_i^t = \frac{R_A^t + R_E^t}{2} \tag{79}$$

where Ant_i^t shows the position of ant i on repetition t. R_A^t is random motion in the selected ant lion by the roulette wheel in repetition t and R_E^t is the random motion around the elite in repetition t.

In addition to the solution search method described previously, the crossover and mutation operators were used to obtain near-optimal solutions. The operator with two-point crossover is illustrated in Fig. 3.

Two crossover points are chosen at random from the parent chromosomes in the two-point crossover. Between these two points on the parent's chromosome, the genes are swapped. Figure 4 illustrates the mutation operator's performance.

This operator substitutes a random number for the selected gene. The genetic algorithm's crossover and mutation operators have been used in accordance with the presented contents and in order to move the ant lions toward the near-optimal solution.

Inputs:

K: *Set of sources*

J: *Set of depots*

P: *Set of Product*

Dem_{jp}: *Demand on depot j of product p*

Cap_k: *Capacity of source k*

Tr_{kj}: *Transportation cost of one unit of product from source k to depot j*

$v(K+J)$: *Encoded solution*

Output:

X_{kjp}: *Quantity of shipment between source k and depot j*

S_{jp}: *Shortage of depot j of product p*

Y_k: *Opening of a center at location k*

***Step* 1.** $For\ p = 1\ to\ P$

$$Select\ a\ node\ on\ l = arg\ max\{v(k),\ \ \forall k \in K\},so \sum_{k \in K} Y_k = l$$

***Step* 2.** $While\ |\{d\}| < l$:

$Select\ a\ node\ on\ d = arg\ max\{v(k), k \in K\}$

$If\ |\{d\}| = l\ then\ v(k-l) = 0,\ \ \forall k \in K, l \in L$

$Tr_{(k-l)j} = inf,\ \ \forall j \in |J|, k \in K, l \in L$

$Cap_{(k-l)} = 0,\ \ \forall k \in K, l \in L$

***Step* 3.** $While\ v(|k| + j) \neq 0, \forall j \in J$

***Step* 4.** $X_{kjp} = 0, S_{jp} = 0,\ \ \forall j \in J, k \in K, p \in P$

***Step* 5.** $Select\ a\ node\ based\ on\ l = arg\ max\{v(p),\ \ p \in |K| + |J|\}, \forall j \in J, k \in K$

***Step* 6.** $If\ l \in k\ a\ source\ is\ selected\ k^* = l$

$Then\ j^* = arg\ min\{Tr_{kj} | v(j) \neq 0\}, \forall j \in J\ \ select\ a\ depot\ with\ minimum\ cost$

$Else\ l \in j\ a\ depot\ is\ selected\ j^* = l$

$Then\ k^* = arg\ min\{Tr_{kj} | v(k) \neq 0\}, \forall k \in K\ select\ a\ source\ with\ minimum\ cost$

***Step* 7.** $Update\ demands\ and\ capacities$

$X_{k^*j^*p} = min(Cap_{k^*}, Dem_{j^*p} + S_{j^*p})$

$Cap_{k^*} = Cap_{k^*} - X_{k^*j^*p}$

$Dem_{j^*p} = Dem_{j^*p} + S_{j^*p} - X_{k^*j^*p}$

***Step* 8.** $If\ Cap_{k^*} = 0\ then\ v(k^*) = 0$

$If\ Dem_{j^*p} = 0\ then\ v(j^*) = 0$

***Step* 9.** $$If \sum_{j,p} X_{kjp} > 0\ then\ Y_k = 1$$

End

Fig. 8 The pseudo-code of decoding the two-echelon SCN

According to (Mirjalili et al. 2017), the ALO algorithm has a computational complexity of O(mn), whereas the GA algorithm has a computational complexity of O(2 mn) (Lobo et al. 2000), where n is the population size and m is the individual size. This is equivalent to the HGALO's computational complexity being O (3 mn). GWO, on the other hand, has an O(mn) computational complexity, whereas HHO has an O(m) computational complexity (Mirjalili et al. 2014; Heidari et al. 2019).

Figure 5 illustrates the proposed HGALO algorithm's flowchart and how to use the two algorithms' operators.

The following section discusses a chromosome that solves the leader–follower SCN design problem.

Leader nodes	I J	J K	K L	L M
chromosome	$(\lvert I\rvert + \lvert J\rvert) * \lvert P\rvert$	$(\lvert J\rvert + \lvert K\rvert) * \lvert P\rvert$	$(\lvert K\rvert + \lvert L\rvert) * \lvert P\rvert$	$(\lvert L\rvert + \lvert M\rvert) * \lvert P\rvert$

Follower nodes	I' J'	J' K'	K' L'	L' M
chromosome	$(\lvert I'\rvert + \lvert J'\rvert) * \lvert P\rvert$	$(\lvert J'\rvert + \lvert K'\rvert) * \lvert P\rvert$	$(\lvert K'\rvert + \lvert L'\rvert) * \lvert P\rvert$	$(\lvert L'\rvert + \lvert M'\rvert) * \lvert P\rvert$

Fig. 9 The final solution of the multi-echelon SCN

Random number in continuous space	0.125	0.362	0.418	0.342	0.599	0.908	0.142
Nodes	1	2	3	4	5	6	7
Random number in continuous space	0.908	0.599	0.418	0.362	0.342	0.142	0.125
Priority in discrete space	6	5	3	2	4	7	1

Fig. 10 An example of shipment in the solution search area

4.1 Designing the chromosome for leader–follower SCN design

As it is shown in Fig. 6, consider an echelon of SCN with ($|K|$) sources, ($|J|$) depots and ($|P|$) products. This chromosome's length is $(|K| + |J|) * |P|$ and each cell's location represents the priorities of each node (Ghahremani et al. 2019). For example, Fig. 6 shows a chromosome with 3 sources, 4 depots, and 2 products. Also, in this figure, the demand of each product for depots, potential capacities for sources, and transportation costs between nodes are shown.

The chromosome is decoded in two steps:

Step 1. For the first product, choose the source with the highest priority. If the potential capacity of the chosen sources exceeds the sum of all warehouse demand, the priority of non-selected sources is reduced to zero. Alternatively, assign the highest priority to non-selected sources. Continue in this manner until the capacity of all selected sources exceeds the demand of all depots.

This step specifies the location of the resources to be selected.

Step 2. Determine the highest-priority position among the nodes. If the node is located between two sources, refer to (A); otherwise (B).

A. Determine the cheapest mode of transport between the selected source and all depots. The optimal flow between two nodes is the smallest of the two (depot demand and source capacity). Reduce the priority of the node to zero if the value of depot demand or source capacity becomes zero.

B. Determine the least expensive mode of transportation between the selected depot and all sources. The optimal flow between two nodes is the smallest of the two (depot demand and source capacity). Reduce the priority of the node to zero if the value of depot demand or source capacity becomes zero.

Step 3. Repeat this process until all priorities are equal to zero.

Finally, repeat the process for all products.

The decoding of the example presented in Fig. 6 is depicted in Fig. 7.

As illustrated in Fig. 7, sources 1 and 2 are located optimally. The following is the pseudo-code for decoding the two-echelon SCN design:

As previously stated, this is a multi-echelon, multi-product, leader–follower SCN design problem, and the initial proposed solution must address these factors. As illustrated in Fig. 9, the priority-based encoding is represented by a matrix, in which M, P, C, I, J, K, and L represent the number of customers, products, raw materials, suppliers, potential DCs, production centers, and potential retailers in the leader SC, respectively. Additionally, I', J', K', and L' denote the number of production centers, suppliers, potential DCs, and potential retailers in the following SC.

The designed leader and follower SCN's search area is discrete, which means that no individual from the population components can have an arbitrary value. Allowable

Step 1. Determine the quantity of customer demand and the products selling price in the leader–follower SC based on random data.

The output of this step: The value of decision variables: $D_{mp}^{L}, D_{mp}^{F}, Pr_{mp}^{L}, Pr_{mp}^{F}$

Step 2. Decode the retailers-customers echelon in the leader-follower SC.

The output of this step: The value of decision variables: $ZL_l, U_{lmp}^{L}, U_{l'mp}^{F}$

Step 3. Decode the DCs-retailers echelon in the leader-follower SC.

The output of this step: The value of decision variables: $ZL_k, S_{klp}^{L}, S_{k'l'p}^{F}$

Step 4. Decode the production centers-DCs echelon in the leader-follower SC.

The output of this step: The value of decision variables: $ZL_j, Y_{jkp}^{L}, Y_{j'k'p}^{F}$

Step 5. Decode the suppliers-production centers' echelon in the leader-follower SC.

The output of this step: The value of decision variables: $ZL_i, X_{ijc}^{L}, X_{i'j'c}^{F}$

Step 6. Decode the objective function based on equation (57).

$$
\begin{aligned}
F_L = & \sum_{l\in L}\sum_{m\in M}\sum_{p\in P} Pr_{mp}^{L}U_{lmp}^{L} - \sum_{i\in I}\sum_{j\in J}\sum_{c\in C}\left(\frac{TrIJ1_{ijc}^{L} + 2TrIJ2_{ijc}^{L} + TrIJ3_{ijc}^{L}}{4}\right)X_{ijc}^{L} \\
& - \sum_{j\in J}\sum_{k\in K}\sum_{p\in P}\left(\frac{TrJK1_{jkp}^{L} + 2TrJK1_{jkp}^{L} + TrJK3_{jkp}^{L}}{4}\right)Y_{jkp}^{L} - \\
& \sum_{j\in J}\sum_{k\in K}\sum_{p\in P}\left(\frac{Pc1_{jp}^{L}+2Pc2_{jp}^{L} + Pc3_{jp}^{L}}{4}\right)Y_{jkp}^{L} - \\
& \sum_{k\in K}\sum_{l\in L}\sum_{p\in P}\left(\frac{TrKL1_{klp}^{L} + 2TrKL1_{klp}^{L} + TrKL3_{klp}^{L}}{4}\right)S_{klp}^{L} - \\
& \sum_{l\in L}\sum_{m\in M}\sum_{p\in P}\left(\frac{TrLM1_{jkp}^{L} + 2TrLM1_{jkp}^{L} + TrLM3_{jkp}^{L}}{4}\right)U_{lmp}^{L} - \\
& \sum_{i\in I} FixI_i ZI_i - \sum_{i\in I} FixJ_j ZJ_j - \sum_{k\in K} FixK_k ZK_k - \sum_{l\in L} FixL_l ZL_l
\end{aligned}
$$

Fig. 11 The pseudo-code of decoding the leader–follower multi-echelon SCN design

values are limited to natural numbers between 1 and N. As a result, the continuous search area in the HGALO algorithm must be changed to a discrete search area. In the solution search area, Fig. 10 illustrates an example of a shipment.

Select the largest number in the continuous space of the chromosome in Fig. 10. This number corresponds to the first gene in the new solution. Continue checking the numbers in this manner until all of them have been checked. Figure 11 illustrates the pseudo-code for decoding the leader–follower multi-echelon SCN design.

5 Numerical results

In the preceding section, we examined how to model the leader–follower SCN problem under uncertain conditions and how to control its uncertainty parameters using a fuzzy programming approach (demand, transportation, and purchase costs). The exact method (using Baron Solver) and algorithms are used in this section to evaluate the model and compare the output variables of the problem. The primary objective of this section is to evaluate the HGALO's efficiency in obtaining the near-optimal solution. As a result, a small sample problem is designed first, followed by the solution of the proposed model using Baron Solver. The problem's sensitivity analysis is also discussed below. After solving the model with meta-heuristic algorithms, the

Table 1 The parameters of the boundaries of production based on uniform distribution

Parameter	Range interval
$FixI_i, FixJ_j, FixK_k, FixL_l$	$\sim U(100000, 120000)$
$CapI_{ic}$	$\sim U(1500, 1800)$
$CapJ_{jp}, CapK_{kp}$	$\sim U(1000, 2000)$
$CapL_{lp}$	$\sim U(500, 700)$
O_{cp}	$\sim U(1, 2)$
b^F_{mpp}	$\sim U(0.3, 1.5)$
b^L_{mpp}	$\sim U(0.4, 1.8)$
d^L_{mp}	$\sim U(0.5, 0.9)$
d^F_{mp}	$\sim U(0.3, 0.8)$
$\widetilde{TrIJ}^L_{ijc}, \widetilde{TrJK}^L_{jkp}, \widetilde{TrKL}^L_{klp}, \widetilde{TrLM}^L_{lmp}$	$\sim \{U(5, 10), U(10, 15), U(15, 20)\}$
$\widetilde{Pc}^L_{jp}$	$\sim \{U(2, 4), U(4, 6), U(6, 8)\}$
$\widetilde{TrIJ}^F_{i'j'c}, \widetilde{TrJK}^F_{j'k'p}, \widetilde{TrKL}^F_{k'l'p}, \widetilde{TrLM}^F_{l'mp}$	$\sim \{U(7, 12), U(12, 18), U(18, 25)\}$
$\widetilde{Pc}^F_{j'p}$	$\sim \{U(3, 5), U(5, 8), U(8, 10)\}$
$\widetilde{a}^F_{mp}$	$\sim \{U(200, 300), U(300, 400), U(400, 500)\}$
$\widetilde{a}^L_{mp}$	$\sim \{U(350, 500), U(550, 700), U(700, 900)\}$

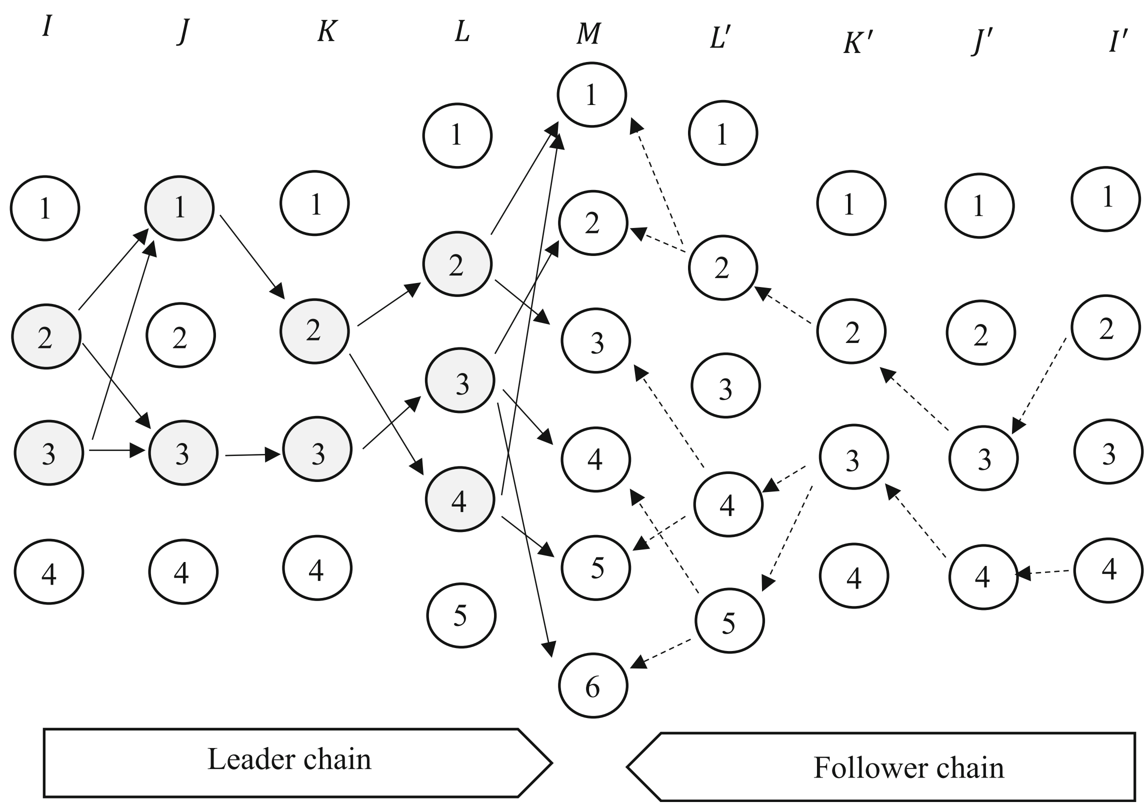

Fig. 12 The location of the potential facilities and allocation between each node

Table 2 The optimal flow between each node in the leader chain

Decision variable	Amount	Decision variable	Amount	Decision variable	Amount	Decision variable	Amount	Decision variable	Amount
$U^{L}_{2,1,1}$	421	$S^{L}_{2,2,1}$	812	$Y^{L}_{1,2,1}$	1205	X^{L}_{211}	1172	$Pr^{L}_{1,1}$	526.19
$U^{L}_{4,1,2}$	405	$S^{L}_{2,2,2}$	665	$Y^{L}_{1,2,2}$	1498	X^{L}_{212}	1207	$Pr^{L}_{1,2}$	424.78
$U^{L}_{2,3,1}$	391	$S^{L}_{2,4,1}$	393	$Y^{L}_{3,3,1}$	1964	X^{L}_{231}	833	$Pr^{L}_{2,1}$	904.07
$U^{L}_{2,3,2}$	665	$S^{L}_{2,4,2}$	833	$Y^{L}_{3,3,2}$	1321	X^{L}_{232}	1386	$Pr^{L}_{2,2}$	909.76
$U^{L}_{3,2,1}$	640	$S^{L}_{3,3,1}$	1964			X^{L}_{331}	1164	$Pr^{L}_{3,1}$	517.13
$U^{L}_{3,2,2}$	497	$S^{L}_{3,3,2}$	1321			X^{L}_{332}	1527	$Pr^{L}_{3,2}$	377.2
$U^{L}_{3,4,1}$	678					X^{L}_{312}	1518	$Pr^{L}_{4,1}$	797.71
$U^{L}_{3,4,2}$	444							$Pr^{L}_{4,2}$	97.76
$U^{L}_{3,6,1}$	646							$Pr^{L}_{5,1}$	523.32
$U^{L}_{3,6,2}$	380							$Pr^{L}_{5,2}$	830.41
$U^{L}_{4,5,1}$	393							$Pr^{L}_{6,1}$	371.22
$U^{L}_{4,5,2}$	428							$Pr^{L}_{6,2}$	144.4

Table 3 The optimal flow between each node in the follower chain

Decision variable	Amount	Decision variable	Amount	Decision variable	Amount	Decision variable	Amount	Decision variable	Amount
$\mathrm{U}^{\mathrm{F}}_{2,1,1}$	318	$\mathrm{S}^{\mathrm{F}}_{2,2,1}$	1014	$\mathrm{Y}^{\mathrm{F}}_{3,2,1}$	1014	$\mathrm{X}^{\mathrm{F}}_{231}$	1014	$\mathrm{Pr}^{\mathrm{L}}_{1,1}$	227.63
$\mathrm{U}^{\mathrm{F}}_{2,1,2}$	637	$\mathrm{S}^{\mathrm{F}}_{2,2,2}$	1120	$\mathrm{Y}^{\mathrm{F}}_{3,2,2}$	1120	$\mathrm{X}^{\mathrm{F}}_{232}$	2240	$\mathrm{Pr}^{\mathrm{L}}_{1,2}$	972.3
$\mathrm{U}^{\mathrm{F}}_{2,2,1}$	696	$\mathrm{S}^{\mathrm{F}}_{3,4,1}$	1119	$\mathrm{Y}^{\mathrm{F}}_{4,3,1}$	1994	$\mathrm{X}^{\mathrm{F}}_{441}$	1994	$\mathrm{Pr}^{\mathrm{L}}_{2,1}$	63.23
$\mathrm{U}^{\mathrm{F}}_{2,2,2}$	483	$\mathrm{S}^{\mathrm{F}}_{3,4,2}$	853	$\mathrm{Y}^{\mathrm{F}}_{4,3,2}$	1624	$\mathrm{X}^{\mathrm{F}}_{442}$	3248	$\mathrm{Pr}^{\mathrm{L}}_{2,2}$	252.57
$\mathrm{U}^{\mathrm{F}}_{4,3,1}$	460	$\mathrm{S}^{\mathrm{F}}_{3,5,1}$	875					$\mathrm{Pr}^{\mathrm{L}}_{3,1}$	624.87
$\mathrm{U}^{\mathrm{F}}_{4,3,2}$	367	$\mathrm{S}^{\mathrm{F}}_{3,5,2}$	771					$\mathrm{Pr}^{\mathrm{L}}_{3,2}$	401.07
$\mathrm{U}^{\mathrm{F}}_{4,5,1}$	659							$\mathrm{Pr}^{\mathrm{L}}_{4,1}$	676.65
$\mathrm{U}^{\mathrm{F}}_{4,5,2}$	486							$\mathrm{Pr}^{\mathrm{L}}_{4,2}$	533.49
$\mathrm{U}^{\mathrm{F}}_{5,4,1}$	404							$\mathrm{Pr}^{\mathrm{L}}_{5,1}$	381.99
$\mathrm{U}^{\mathrm{F}}_{5,4,2}$	383							$\mathrm{Pr}^{\mathrm{L}}_{5,2}$	440.15
$\mathrm{U}^{\mathrm{F}}_{5,6,1}$	471							$\mathrm{Pr}^{\mathrm{L}}_{6,1}$	280.67
$\mathrm{U}^{\mathrm{F}}_{5,6,2}$	388							$\mathrm{Pr}^{\mathrm{L}}_{6,2}$	326.45

performance of the HGALO algorithm is compared to that of the GA, GWO, ALO, and HHO algorithms.

5.1 Solving the small size sample problem

A small sample problem is designed in this subsection to evaluate the presented model and compare the output variables. It encompasses two distinct product categories, two distinct raw material categories, four suppliers, four manufacturing facilities, four distribution centers, five retailers, and six customers.

Due to the lack of available benchmarks in the literature, random data from a uniform distribution is generated using the MATLAB software, as illustrated in Table 1.

Due to the model's nonlinearity, Solver Baron is used on the GAMS 24.8.5 software. The numbers and locations of potential facilities, as well as the optimal flow between each node, are shown in Fig. 12 and Tables 2 and 3,

Table 4 Changing of the OBFV through adjustment of the uncertainty rates

Uncertainty rates ($\alpha = \beta$)	OBFV	Average selling price of products (leader chain)	Average selling price of products (follower chain)
0.9	1927883.3	500.71	397.56
0.8	1934265.5	507.87	410.97
0.7	1943648.4	516.90	418.74
0.6	1964793.3	525.17	423.94
0.5	1989577.9	535.32	431.75
0.4	2027543.2	545.67	440.34
0.3	2063654.2	550.94	453.17
0.2	2094678.5	555.47	462.84
0.1	2124876.8	556.24	473.67

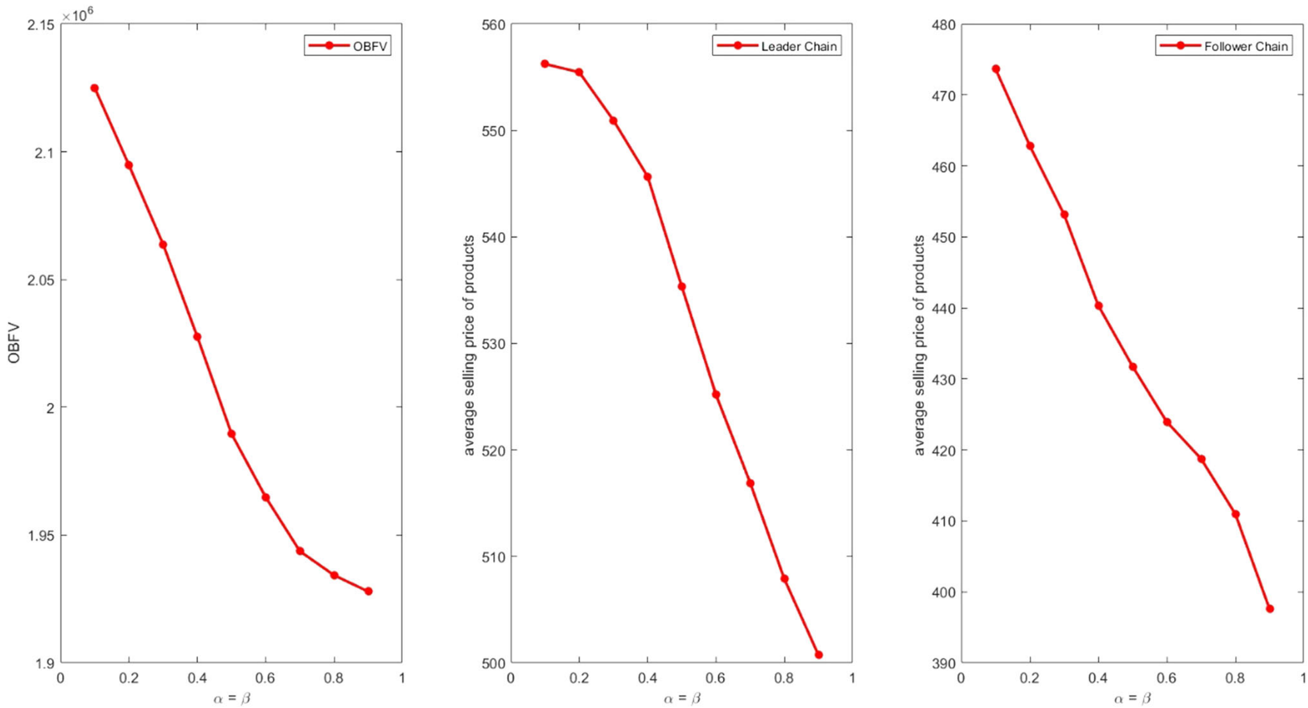

Fig. 13 Changes in the OBFV and average selling price of products by changing the uncertainty rates

respectively, when uncertainty rates ($\alpha = \beta = 0.5$) are taken into account.

According to Fig. 12, the optimal locations are suppliers with numbers 2 and 3, production centers with numbers 1 and 3, distribution centers with numbers 2 and 3, and retailers with numbers 2, 3, and 4. The objective function value (OBFV) of the proposed model is 1989577.94, and the optimal flow between each leader–follower chain is shown in Tables 2 and 3. Additionally, this table shows the prices charged by retailers in the leader–follower chain.

5.2 Sensitivity analysis

After verifying and validating the proposed model, it is necessary to analyze its sensitivity. To do so, an uncertainty rate is chosen, and the resulting changes in the OBFV are shown in Table 4.

According to Table 4, as the uncertainty rate increases, the demand for products increases, while the OBFV and average selling price of products decrease. Figure 13 depicts the trend of changes in OBFV at various levels of uncertainty.

Table 5 The value of proposed and optimized parameters of meta-heuristic algorithms

Algorithm	Parameter	Level one	Level two	Level three	Optimum level
GA	Maxit	50	100	200	200
	$N-\mathrm{pop}$	50	100	200	100
	P_c	0.7	0.8	0.9	0.7
	P_m	0.03	0.05	0.07	0.05
HGALO	Maxit	50	100	200	200
	$\mathrm{N-ant}$	50	100	200	100
	b_i	500	1000	1500	1500
	a_i	200	300	400	400
	P_c	0.7	0.8	0.9	0.8
	P_m	0.03	0.05	0.07	0.05
ALO	Maxit	50	100	200	200
	$N-\mathrm{ant}$	50	100	200	200
	b_i	500	1000	1500	1000
	a_i	200	300	400	300
GWO	Maxit	50	100	200	200
	$N-\mathrm{Wolf}$	50	100	200	200
	A	1	2	3	3
	C	1	2	3	2
HHO	Maxit	50	100	200	200
	$N-\mathrm{pop}$	50	100	200	100
	Strategyrate	*0.05*	*0.1*	*0.15*	*0.05*

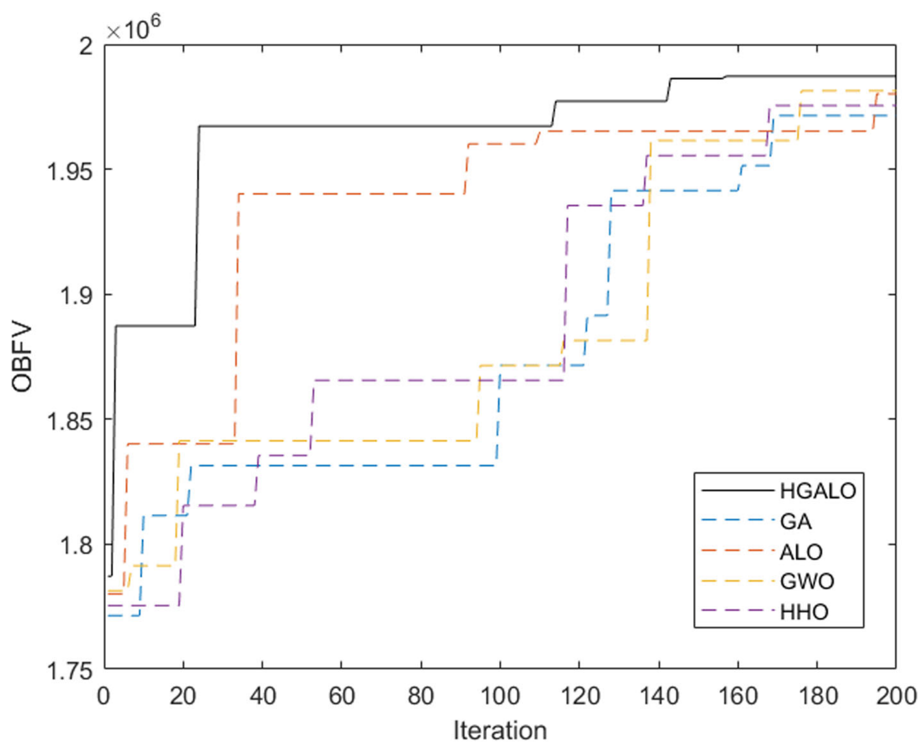

Fig. 14 The convergence of the algorithms in achieving the OBFV

Table 6 The OBFV obtained from different solution approaches

Algorithm	OBFV	Gap between baron solver and algorithms (%)	CPU-time
Baron solver	1989577.94	–	84.25
HGALO	1989398.88	0.009	33.14
GA	1989100.44	0.024	27.26
ALO	1989458.57	0.006	25.94
GWO	1989299.40	0.014	20.34
HHO	1989219.82	0.018	26.47

Table 7 The optimal location and number of facilities obtained from different solution methods

Algorithm	Suppliers	Production centers	DCs	Retailers
Baron solver	2–3	1–3	2–3	2–3–4
HGALO	2–3	1–3	2–3	2–3–4
GA	1–3	1–3	2–3	2–3–4
ALO	2–3	1–3	1–3	1–3–4
GWO	1–3	2–3	2–3	2–3–4
HHO	1–2	1–3	2–3	2–3–4

Table 8 The Average selling price of products (leader and follower chain) obtained from different solution methods

Algorithm	Average selling price of products (leader chain)	Average selling price of products (follower chain)
Baron solver	535.32	431.75
HGALO	535.72	430.17
GA	535.24	429.37
ALO	536.14	431.20
GWO	534.94	430.25
HHO	534.86	430.86

Table 9 The sample problems size

Sample problem no	I	J	K	L	M	P	C
1	5	5	5	7	8	3	2
2	7	6	6	8	10	3	2
3	8	7	7	10	12	3	2
4	9	8	8	12	15	4	2
5	10	10	10	14	18	4	3
6	12	12	12	16	21	4	3
7	15	14	14	18	23	5	3
8	18	16	16	20	25	5	4
9	20	18	18	22	28	5	4
10	25	20	20	25	30	6	4

5.2.1 Tuning the meta-heuristics algorithms by Taguchi method

Prior to solving the problem with meta-heuristic algorithms, the Taguchi method was used to tune the parameters of the GA, HGALO, ALO, HHO, and GWO algorithms. Prior to beginning the Taguchi process, it is necessary to identify the relevant factors. Then, the appropriate levels for each factor should be determined, followed by the appropriate test design for these control factors. After establishing the design of the experiment, the experiments are conducted and the results are analyzed to determine the optimal parameter combination. Three levels are considered in this paper for each factor in accordance with Table 5. We can determine the design and implementation of experiments for each algorithm by considering the number of factors and the numbers of their levels. Given that the proposed model is a single objective function, we use the RPD index to tune the parameters during the data analysis.

$$\mathrm{RPD} = \frac{\mathrm{Best}^*_{\mathrm{sol}} - \mathrm{Algorithm}_{\mathrm{sol}}}{\mathrm{Best}^*_{\mathrm{sol}}}. \tag{80}$$

5.2.2 Solving sample problems in small size

This subsection evaluates the meta-heuristic algorithms used to solve the previous section's small size example. The purpose of this analysis is to determine how algorithms converge toward a near-optimal solution and its output variables. Thus, a sample problem is considered that includes two types of products, two types of raw materials, four suppliers, four manufacturing centers, four distribution centers, five retailers, and six customers. After solving the numerical example using meta-heuristic algorithms, the algorithms' convergence toward achieving the OBFV is determined, as illustrated in Fig. 14.

As illustrated in Fig. 14, the HGALO algorithm converges faster and has a greater OBFV than other algorithms. Table 6 shows the OBFV obtained by solving a numerical example and comparing it to Baron's solver.

Table 10 OBFV obtained from solving sample problems, using different solution methods

Sample problem	OBFV					
	HGALO	GA	ALO	GWO	HHO	(Baron solver)
1	2416876.1	2415789.6	2416556.7	2415824.2	2416090.5	2427541.6
2	2826497.4	2824613.6	2824700.6	2824796.6	2826164.8	2846237.1
3	3124685.5	3124259.7	3124555.6	3131394.7	3124664.3	3147820.3
4	3264975.6	3261974.3	3262077.7	3264291.1	3263119.5	–
5	3478945.7	3471165.1	3477121.3	3477352.2	3472619.1	–
6	3864472.3	3854687.7	3859479.8	3859047.6	3861011.6	–
7	3947651.2	3924686.4	3950976.8	3942017.6	3931025.3	–
8	4157666.4	4111794.6	4142973.8	4141845.1	4159253.9	–
9	4268794.3	4213428.6	4220017.0	4241020.9	4266565.5	–
10	4378261.4	4304789.8	4325278.2	4350018.1	4364981.6	–
Mean	3571554.6	3550718.9	3560373.7	3564760.8	3569877.5	

Sample problem	RPD (%)					
	HGALO	GA	ALO	GWO	HHO	(Baron solver)
1	0.000	0.045	0.013	0.044	0.033	–
2	0.000	0.067	0.064	0.060	0.012	–
3	0.214	0.228	0.218	0.000	0.215	–
4	0.000	0.092	0.089	0.021	0.057	–
5	0.000	0.224	0.052	0.046	0.182	–
6	0.000	0.253	0.129	0.140	0.090	–
7	0.084	0.665	0.000	0.227	0.505	–
8	0.038	1.141	0.391	0.419	0.000	–
9	0.000	1.297	1.143	0.651	0.052	–
10	0.000	1.678	1.210	0.645	0.303	–

Table 11 CPU-time obtained from solving sample problems, using different solution methods

Sample problem	HGALO	GA	ALO	GWO	HHO	(Baron solver)
1	67.1	54.4	55.5	46.4	52.4	126.47
2	71.2	58.6	65.4	56.6	62.3	347.68
3	80.3	69.8	80.4	67.3	73.5	846.82
4	91.7	80.6	94.7	85.2	88.4	>1000
5	112.3	99.3	120.4	110.3	109.2	>1000
6	140.4	122.3	148.5	134.1	134.5	>1000
7	170.6	152.3	187.0	181.3	167.7	>1000
8	210.3	190.0	237.6	229.8	208.0	>1000
9	261.7	235.4	292.7	281.3	258.4	>1000
10	328.7	290.7	364.0	353.1	329.4	>1000
Mean	153.4	135.3	164.6	154.5	148.3	>1000

According to the results of Table 6, the maximum gap is equal to 0.024 percent, indicating the algorithms' high efficiency in achieving the OBFV in less time than the Baron Solver. Additionally, the results indicate that meta-heuristic algorithms solve problems 60% faster than Baron Solver.

The optimal location and number of facilities for solving small numerical examples are shown in Table 7.

According to Table 7, all solution methods produce the same number of optimal locations. Finally, Table 8 illustrates the average selling price of products (Leader and Follower chains) when the uncertainty rate is set to 0.5.

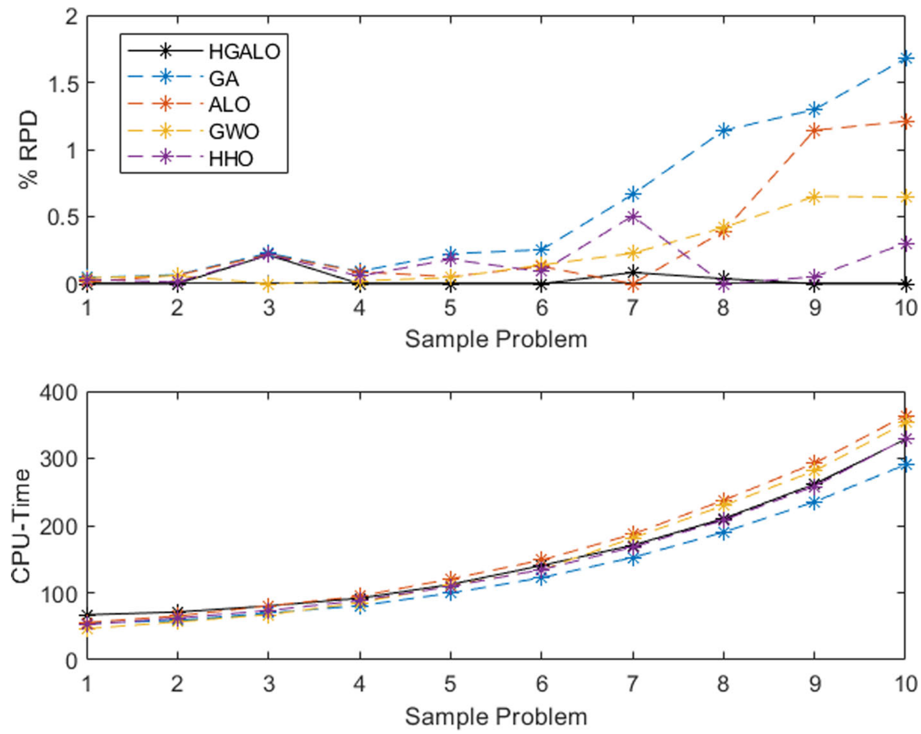

Fig. 15 Changes in averages of the RPD % and CPU-time in large sample sizes

Table 12 *T* Test outputs at 95% confidence level

Algorithm	Index	Means different	Confidence interval 95%		*T* value	*P* value
			Lower bound	Upper bound		
GA-HGALO	OBFV	20,836	3725	37,946	2.75	**0.022**
GA-ALO		9655	1212	18,097	2.59	**0.029**
GA-GWO		14,042	2980	25,104	2.87	**0.018**
GA-HHO		19,159	− 634	38,951	2.19	0.056
ALO-HGALO		11,181	− 1819	24,181	1.95	0.084
ALO-GWO		4387	− 3134	11,908	1.32	0.220
ALO-HHO		9504	− 6948	25,955	1.31	0.224
GWO-HGALO		6794	− 349	13,936	2.15	0.060
GWO-HHO		5117	− 4678	14,911	1.18	0.268
HHO-HGALO		1677	− 3592	6946	0.72	0.490
GA-HGALO	CPU-time	18.09	11.96	24.21	6.679	**0.000**
GA-ALO		29.28	12.35	46.21	3.91	**0.004**
GA-GWO		19.20	2.18	36.22	2.55	**0.031**
GA-HHO		13.04	4.69	21.39	3.53	**0.006**
ALO-HGALO		11.19	− 0.19	22.57	2.22	0.053
ALO-GWO		10.08	8.272	11.88	12.61	**0.000**
ALO-HHO		16.24	7.28	25.20	4.10	**0.003**
GWO-HGALO		1.11	− 10.47	12.69	0.22	0.833
GWO-HHO		6.16	− 3.03	15.35	1.52	0.164
HHO-HGALO		5.05	1.97	8.13	3.71	**0.005**

Additionally, the results of Table 8 demonstrate the close proximity of the average selling prices of products (leader and follower chains) obtained using various solution methods in comparison with the Baron Solver.

5.2.3 Solving sample problems in large size

After evaluating the meta-heuristic algorithms, this subsection solves the leader–follower model using the

Table 13 Algorithm performance ranking results

Algorithm	Mean of OBFV	Mean of CPU-time	Utility weight	Rank
HGALO	3,571,554.6	153.43	0.6435	1
GA	3,550,718.9	135.34	0.4618	5
ALO	3,560,373.7	164.62	0.5218	4
GWO	3,564,760.8	154.54	0.5517	3
HHO	3,569,877.5	148.38	0.5611	2

HGALO, GA, ALO, GWO, and HHO algorithms. As a result, ten sample problems of varying sizes are designed to evaluate the performance of the proposed algorithms. Tables 9, 10, and 11 illustrate the size of the exemplified problems and the OBFV and CPU-time of the proposed algorithms (11).

According to the results of Tables 9, 10, and 11, the exact solution cannot be found by increasing the size of the problem. It is obvious that the CPU-time required to solve the model using the exact method is quite high, as the third sample problem requires 846.82 s. By comparing the meta-heuristic algorithms for solving large-scale sample problems, it is possible to deduce that the OBFV obtained from the HGALO algorithm was superior to the other algorithms in all sample problems. Additionally, when the RPD index of the algorithms is compared, it is observed that as the size of the problem increases, the GA algorithm loses its ability to obtain a near-optimal solution. Simultaneously, it consumes less CPU-time than the other algorithms.

Figure 15 illustrates the changes in the OBFV and CPU-time averages as a result of the proposed meta-heuristics algorithms in all sample problems.

The T Test was used at a 95% confidence level to compare the significant difference between the OBFV and CPU-time obtained from the proposed algorithms. If the P value is less than 0.05, the hypothesis test indicates that there is a significant difference in the averages of that computational index between the algorithms used. *T* Test output results for large sample size problems using these algorithms are shown in Table 12.

The P value for the OBFV index is less than 0.05, indicating a significant difference between the averages of the OBFV index for the GA–HGALO, GA–ALO, and GA–GWO algorithms. Additionally, there is no discernible difference in the averages of this index between the other algorithms. Due to a lack of decision-making regarding the most efficient algorithm for solving the proposed mathematical model, the TOPSIS method for ranking algorithms has been discussed using two indicators of OBFV and CPU-time. The results of these comparisons are shown in Table 13.

According to the results in Table 13, the HGALO algorithm obtained the optimal value of the objective function when compared to other algorithms. While the GA algorithm took less time to solve the model than other algorithms. However, based on the TOPSIS ranking results, it is observed that the HGALO algorithm, with a utility weight of 0.6435, is more efficient than other algorithms when both OBFV and CPU-time are considered. Apart from the scientific findings, the proposed model has the strongest correlation with the activities of companies manufacturing electronic and automotive components in the global SC. Within these networks, manufacturing firms compete fiercely for market share and product pricing. As a result, large and small businesses compete against one another under the leader and follower chains, respectively. Under conditions of uncertainty, the model presented in this paper can provide beneficial management results for managers of companies that manufacture electronic and automotive components, enabling managers to make appropriate decisions about product pricing, volume of production, distribution, and facility location.

6 Conclusion

The purpose of this paper was to develop a new leader–follower SCN model that maximizes both the leader and follower chains' profits. In the leader and follower SC, four echelons (suppliers, manufacturers, distribution centers, and retailers) are considered, and they compete for product pricing in the market (customers). The high degree of complexity associated with pricing the two leader and follower chains is a result of the uncertainty surrounding the amount of potential market demand. Special tools such as fuzzy programming are used to control the potential demand parameters and the transportation costs of products and raw materials between different echelons of the chain network. The difference between the leader and follower chain networks in this paper is due to strategic decisions made in the leader chain. The location of facilities at all potential centers, such as suppliers, manufacturers, distribution centers, and retailers, should be made part of the leader chain's strategic planning. The tactical decisions made in the leader and follower chains concern the optimal flow of products and raw materials between the two SCN echelons. Finally, operational decisions include pricing final products in the market (for customers) by leader and follower chains in order to maximize profit in the face of uncertainty.

In this paper, the KKT method is used to convert a bi-level mathematical model to a one-level mathematical model. Due to the NP-Hard nature of location and SCN design problems, this paper employs a novel hybrid of genetic algorithm (GA) and ant-lion optimization algorithm (ALO) to solve the problem. The ant-lion optimization algorithm operators design the problem's chromosome, locate potential facilities, and optimally allocate products between the different echelons of the leader and follower chains, while the genetic algorithm operators price the products in the market. Finally, statistical comparisons between the developed algorithm and the genetic algorithm are performed. According to the findings, as the uncertainty rate increases, demand also increases, while the OBFV and average selling price of products decrease. By comparing the meta-heuristic algorithms for solving large-size sample problems, it is possible to deduce that the OBFV obtained from the HGALO algorithm was superior to the GA algorithm in all sample problems. Additionally, the P value for both the OBFV and the OBFV is less than 0.05, indicating a significant difference between the averages of this index in the GA–HGALO, GA–ALO, and GA–GWO algorithms. Finally, the high OBFV of the HGALO algorithm in solving sample problems demonstrates the algorithm's superior efficiency in comparison with other algorithms. In addition to the proposed algorithm, other novel algorithms such as the whale optimization algorithm, the slap swarm algorithm, and others may be used to solve the introduced model. Additionally, it is suggested that researchers consider the facility location problem in the follower's model and control the uncertainty parameters using a robust possibilistic optimization method. Additionally, researchers can use a permutation-based encoding to encode the solution.

Appendix

Convexity conditions are established using continuous decision variables and linear equations for the follower's constraints, and thus we wish to establish the concavity of the follower's OBFV in the following manner:

Lemma *OBFV f_F is concave.*

Proof We can prove the concavity of f_F by negative definite Hessian matrix. It is necessary to demonstrate the concavity of the first nonlinear statement of f_F using the summation rule for multiple concave functions, as well as the concavity of the other statements' summation. Thus, if *m = 2* and *r = 2*, the OBFV's first term is presented as follows using the Hessian matrix.

$$P_{11}D_{11} + P_{12}D_{12} + P_{21}D_{21} + P_{22}D_{22}.$$

The above statements considering the equations, can be replaced with their equals. Next, the following Hessian matrix can be proved for $P_{11}, P_{12}, P_{21}, P_{22}D_{22}$ as below:

$$H = \begin{bmatrix} -2b_{111}^F & -b_{121}^F - b_{112}^F & 0 \quad 0 & \\ -b_{121}^F - b_{112}^F & -2b_{122}^F & 0 \quad 0 & \\ 0 \quad 0 & & -2b_{211}^F & -b_{221}^F - b_{212}^F \\ 0 \quad 0 & & -b_{221}^F - b_{212}^F & -2b_{222}^F \end{bmatrix}.$$

Then, we have eigenvalues:

$$\mathrm{eig}(H) = \begin{bmatrix} -b_{111}^F - b_{122}^F - \sqrt{{b_{111}^F}^2 + {b_{112}^F}^2 + {b_{121}^F}^2 + {b_{122}^F}^2 - 2\left(b_{111}^F\right)\left(b_{122}^F\right) + 2\left(b_{121}^F\right)\left(b_{112}^F\right)} \le 0 \\ -b_{211}^F - b_{222}^F - \sqrt{{b_{211}^F}^2 + {b_{212}^F}^2 + {b_{221}^F}^2 + {b_{222}^F}^2 - 2\left(b_{211}^F\right)\left(b_{222}^F\right) + 2\left(b_{221}^F\right)\left(b_{212}^F\right)} \le 0 \\ -b_{111}^F - b_{122}^F - \sqrt{{b_{111}^F}^2 + {b_{112}^F}^2 + {b_{121}^F}^2 + {b_{122}^F}^2 - 2\left(b_{111}^F\right)\left(b_{122}^F\right) + 2\left(b_{121}^F\right)\left(b_{112}^F\right)} \le 0 \\ -b_{211}^F - b_{222}^F - \sqrt{{b_{211}^F}^2 + {b_{212}^F}^2 + {b_{221}^F}^2 + {b_{222}^F}^2 - 2\left(b_{211}^F\right)\left(b_{222}^F\right) + 2\left(b_{221}^F\right)\left(b_{212}^F\right)} \le 0 \end{bmatrix}.$$

The first three rows of $eig(H)$ are negative. So, we will apply the negativity for the last three rows, if:

$$
\begin{aligned}
& -b_{111}^F - b_{122}^F \\
& - \sqrt{{b_{111}^F}^2 + {b_{112}^F}^2 + {b_{121}^F}^2 + {b_{122}^F}^2 - 2\left(b_{111}^F\right)\left(b_{122}^F\right) + 2\left(b_{121}^F\right)\left(b_{112}^F\right)} \\
& \leq 0
\end{aligned}
$$

$$
\begin{aligned}
& -b_{211}^F - b_{222}^F \\
& - \sqrt{{b_{211}^F}^2 + {b_{212}^F}^2 + {b_{221}^F}^2 + {b_{222}^F}^2 - 2\left(b_{211}^F\right)\left(b_{222}^F\right) + 2\left(b_{221}^F\right)\left(b_{212}^F\right)} \\
& \leq 0.
\end{aligned}
$$

That means:

$$
{b_{112}^F}^2 + {b_{121}^F}^2 \leq 2\left(b_{111}^F\right)\left(b_{122}^F\right)
$$

$$
{b_{212}^F}^2 + {b_{221}^F}^2 \leq 2\left(b_{211}^F\right)\left(b_{222}^F\right).
$$

As a result of the negative eigenvalues of the Hessian matrix, the follower's OBFV f_F will be concave if the sum of the self-price coefficients multiplied by two is greater than the square of the complementary coefficient's sum. In light of these conditions, the results indicate that all problem sizes exhibit concavity of the lower-level OBFV.

Funding The authors have not disclosed any funding.

Data availability Enquiries about data availability should be directed to the authors.

Declarations

Conflict of interest The authors have not disclosed any competing interests.

References

Amiri AS, Torabi SA, Ghodsi R (2018) An iterative approach for a bi-level competitive supply chain network design problem under foresight competition and variable coverage. Transp Res Part E Logist Transp Rev 109:99–114

Boronoos M, Mousazadeh M, Torabi SA (2021) A robust mixed flexible-possibilistic programming approach for multi-objective closed-loop green supply chain network design. Environ Dev Sustain 23(3):3368–3395

Cai GG, Chiang WC, Chen X (2011) Game theoretic pricing and ordering decisions with partial lost sales in two-stage supply chains. Int J Prod Econ 130(2):175–185

Davis PS, Ray TL (1969) A branch-bound algorithm for the capacitated facilities location problem. Naval Res Log Q 16(3):331–344

Farahani RZ, Rezapour S, Drezner T, Fallah S (2014) Competitive supply chain network design: an overview of classifications, models, solution techniques and applications. Omega 45:92–118

Ghahremani-Nahr J, Kian R, Sabet E (2019) A robust fuzzy mathematical programming model for the closed-loop supply chain network design and a whale optimization solution algorithm. Expert Syst Appl 116:454–471

Ghomi-Avili M, Naeini SGJ, Tavakkoli-Moghaddam R, Jabbarzadeh A (2018) A fuzzy pricing model for a green competitive closed-loop supply chain network design in the presence of disruptions. J Clean Prod 188:425–442

Ghomi-Avili M, Tavakkoli-Moghaddam R, Jalali Naeini SG, Jabbarzadeh A (2020) Competitive green supply chain network design model considering inventory decisions under uncertainty: a real case of a filter company. Int J Prod Res 59:1–20

Gümüş ZH, Floudas CA (2005) Global optimization of mixed-integer bilevel programming problems. CMS 2(3):181–212

Hasani AA (2016) Competitive supply chain network design considering marketing strategies: a hybrid metaheuristic algorithm. Int J Supply Oper Manag 3(3):1429

Heidari AA, Mirjalili S, Faris H, Aljarah I, Mafarja M, Chen H (2019) Harris hawks optimization: algorithm and applications. Futur Gener Comput Syst 97:849–872

Jayaraman V, Patterson RA, Rolland E (2003) The design of reverse distribution networks: models and solution procedures. Eur J Oper Res 150(1):128–149

Keshavarz-Ghorbani F, Arshadi Khamseh A (2022) Modeling and optimizing a multi-period closed-loop supply chain for pricing, warranty period, and quality management. J Ambient Intell Humanized Comput 13(4):2061–2089

Kurata H, Yao DQ, Liu JJ (2007) Pricing policies under direct vs. indirect channel competition and national vs. store brand competition. Eur J Oper Res 180(1):262–281

Leng M, Parlar M (2010) Game-theoretic analyses of decentralized assembly supply chains: Non-cooperative equilibria vs coordination with cost-sharing contracts. Eur J Oper Res 204(1):96–104

Li D, Nagurney A (2017) Supply chain performance assessment and supplier and component importance identification in a general competitive multitiered supply chain network model. J Global Optim 67(1–2):223–250

Li J, Yi Y, Yang H (2020) Information investment and sharing in a two-echelon supply chain under government subsidy and consumer preference for energy-saving products. Math Prob Eng 2020:1–8

Liu B, Zhang R, Xiao M (2010) Joint decision on production and pricing for online dual channel supply chain system. Appl Math Model 34(12):4208–4218

Liu Z, Zheng XX, Li DF, Liao CN, Sheu JB (2021) A novel cooperative game-based method to coordinate a sustainable supply chain under psychological uncertainty in fairness concerns. Transp Res Part E Log Transp Rev 147:102237

Lobo FG, Goldberg DE, Pelikan M (2000) Time complexity of genetic algorithms on exponentially scaled problems. In: Proceedings of the 2nd annual conference on genetic and evolutionary computation, pp 151–158

Mirjalili S (2015) The ant lion optimizer. Adv Eng Softw 83:80–98

Mirjalili S, Mirjalili SM, Lewis A (2014) Grey wolf optimizer. Adv Eng Softw 69:46–61

Mirjalili S, Jangir P, Saremi S (2017) Multi-objective ant lion optimizer: a multi-objective optimization algorithm for solving engineering problems. Appl Intell 46(1):79–95

Mokhlesian M, Zegordi SH (2014) Application of multidivisional bi-level programming to coordinate pricing and inventory decisions in a multiproduct competitive supply chain. Int J Adv Manuf Technol 71(9–12):1975–1989

Mozafari, M., Naimi-Sadigh, A., & Seddighi, A. H. (2021). Possibilistic cooperative advertising and pricing games for a two-echelon supply chain. Soft Computing, 1–15.

Nagurney A (2021) Supply chain game theory network modeling under labor constraints: applications to the Covid-19 pandemic. Eur J Oper Res 293:880–891

Nobari A, Kheirkhah AS, Esmaeili M (2019) Considering chain to chain competition in forward and reverse logistics of a dynamic and integrated supply chain network design problem. J Ind Syst Eng 12(1):147–166

Noh J, Kim JS, Sarkar B (2019) Two-echelon supply chain coordination with advertising-driven demand under Stackelberg game policy. Eur J Ind Eng 13(2):213–244

Nozari H, Ghahremani-Nahr J, Szmelter-Jarosz A (2022) A multi-stage stochastic inventory management model for transport companies including several different transport modes. Int J Manag Sci Eng Manag. https://doi.org/10.1080/17509653.2022.2042747

Pritchard D (2007) The Lemke–Howson algorithm. In:CO 456—game theory F07, David Pritchard—Notes 2 1

Rezapour S, Farahani RZ, Fahimnia B, Govindan K, Mansouri Y (2015) Competitive closed-loop supply chain network design with price-dependent demands. J Clean Prod 93:251–272

Saberi S, Cruz JM, Sarkis J, Nagurney A (2018) A competitive multiperiod supply chain network model with freight carriers and green technology investment option. Eur J Oper Res 266(3):934–949

Saghaeeian A, Ramezanian R (2018) An efficient hybrid genetic algorithm for multiproduct competitive supply chain network design with price-dependent demand. Appl Soft Comput 71:872–893

Sarkar S, Bhadouriya A (2020) Manufacturer competition and collusion in a two-echelon green supply chain with production trade-off between non-green and green quality. J Clean Prod 253:119904

Sazvar Z, Zokaee M, Tavakkoli-Moghaddam R, Salari SAS, Nayeri S (2021) Designing a sustainable closed-loop pharmaceutical supply chain in a competitive market considering demand uncertainty, manufacturer's brand and waste management. Ann Oper Res 2021:1–32

Szmelter-Jarosz A, Ghahremani-Nahr J, Nozari H (2021) A neutrosophic fuzzy optimisation model for optimal sustainable closed-loop supply chain network during COVID-19. J Risk Financ Manag 14(11):519

Tang S, Wang W, Zhou G (2020) Remanufacturing in a competitive market: A closed-loop supply chain in a Stackelberg game framework. Expert Syst Appl 161:113655

Wang D, Du G, Jiao RJ, Wu R, Yu J, Yang D (2016) A Stackelberg game theoretic model for optimizing product family architecting with supply chain consideration. Int J Prod Econ 172:1–18

Wu CH, Chen CW, Hsieh CC (2012) Competitive pricing decisions in a two-echelon supply chain with horizontal and vertical competition. Int J Prod Econ 135(1):265–274

Yildizbaşi A, Çalik A, Paksoy T, Farahani RZ, Weber GW (2018) Multi-level optimization of an automotive closed-loop supply chain network with interactive fuzzy programming approaches. Technol Econ Dev Econ 24(3):1004–1028

Yue D, You F (2017) Stackelberg-game-based modeling and optimization for supply chain design and operations: a mixed integer bilevel programming framework. Comput Chem Eng 102:81–95

Zhang X, Huang GQ (2010) Game-theoretic approach to simultaneous configuration of platform products and supply chains with one manufacturing firm and multiple cooperative suppliers. Int J Prod Econ 124(1):121–136

Zhang X, Chan FT, Adamatzky A, Mahadevan S, Yang H, Zhang Z, Deng Y (2017) An intelligent physarum solver for supply chain network design under profit maximization and oligopolistic competition. Int J Prod Res 55(1):244–263

Ziari M, Sajadieh MS (2022) A joint pricing and network design model for a closed-loop supply chain under disruption (glass industry). RAIRO-Operations Res 56(1):431–444